



# Genome Evolution of Two Genetically Homogeneous Infectious Bursal Disease Virus Strains During Passages *in vitro* and *ex vivo* in the Presence of a Mutagenic Nucleoside Analog

## OPEN ACCESS

### Edited by:

Daniel Roberto Perez,  
University of Georgia, United States

### Reviewed by:

Rafael Elias Marques,  
National Center for Research  
in Energy and Materials, Brazil  
Jae-Keun Park,  
National Institutes of Health (NIH),  
United States  
LC, National Center for Research  
in Energy and Materials, Brazil in  
collaboration with reviewer RM

### \*Correspondence:

Sébastien Mathieu Soubies  
sebastien.soubies@anses.fr

### Specialty section:

This article was submitted to  
Virology,  
a section of the journal  
Frontiers in Microbiology

**Received:** 09 March 2021

**Accepted:** 14 May 2021

**Published:** 11 June 2021

### Citation:

Cubas-Gaona LL, Flageul A, Courtyllon C, Briand F-X, Contrant M, Bougeard S, Lucas P, Quenault H, Leroux A, Keita A, Amelot M, Grasland B, Blanchard Y, Eterradossi N, Brown PA and Soubies SM (2021) Genome Evolution of Two Genetically Homogeneous Infectious Bursal Disease Virus Strains During Passages *in vitro* and *ex vivo* in the Presence of a Mutagenic Nucleoside Analog. *Front. Microbiol.* 12:678563. doi: 10.3389/fmicb.2021.678563

Liliana L. Cubas-Gaona<sup>1</sup>, Alexandre Flageul<sup>1</sup>, Céline Courtyllon<sup>1</sup>, Francois-Xavier Briand<sup>1</sup>, Maud Contrant<sup>2</sup>, Stephanie Bougeard<sup>3</sup>, Pierrick Lucas<sup>2</sup>, Hélène Quenault<sup>2</sup>, Aurélie Leroux<sup>2</sup>, Alassane Keita<sup>4</sup>, Michel Amelot<sup>4</sup>, Béatrice Grasland<sup>1</sup>, Yannick Blanchard<sup>2</sup>, Nicolas Eterradossi<sup>1</sup>, Paul Alun Brown<sup>1</sup> and Sébastien Mathieu Soubies<sup>1\*</sup>

<sup>1</sup> Avian and Rabbit Virology, Immunology and Parasitology Unit (VIPAC), French Agency for Food, Environmental and Occupational Health Safety (ANSES), Ploufragan, France, <sup>2</sup> Viral Genetics and Biosecurity Unit (GVB), French Agency for Food, Environmental and Occupational Health Safety (ANSES), Ploufragan, France, <sup>3</sup> Epidemiology, Animal Health and Welfare Unit (EPISABE), French Agency for Food, Environmental and Occupational Health Safety (ANSES), Ploufragan, France, <sup>4</sup> Experimental Poultry Unit (SELEAC), French Agency for Food, Environmental and Occupational Health Safety (ANSES), Ploufragan, France

The *avibirnavirus* infectious bursal disease virus (IBDV) is responsible for a highly contagious and sometimes lethal disease of chickens (*Gallus gallus*). IBDV genetic variation is well-described for both field and live-attenuated vaccine strains, however, the dynamics and selection pressures behind this genetic evolution remain poorly documented. Here, genetically homogeneous virus stocks were generated using reverse genetics for a very virulent strain, rvv, and a vaccine-related strain, rCu-1. These viruses were serially passaged at controlled multiplicities of infection in several biological systems, including primary chickens B cells, the main cell type targeted by IBDV *in vivo*. Passages were also performed in the absence or presence of a strong selective pressure using the antiviral nucleoside analog 7-deaza-2'-C-methyladenosine (7DMA). Next Generation Sequencing (NGS) of viral genomes after the last passage in each biological system revealed that (i) a higher viral diversity was generated in segment A than in segment B, regardless 7DMA treatment and viral strain, (ii) diversity in segment B was increased by 7DMA treatment in both viruses, (iii) passaging of IBDV in primary chicken B cells, regardless of 7DMA treatment, did not select cell-culture adapted variants of rvv, preserving its capsid protein (VP2) properties, (iv) mutations in coding and non-coding regions of rCu-1 segment A could potentially associate to higher viral fitness, and (v) a specific selection, upon 7DMA addition, of a Thr329Ala substitution occurred in the viral polymerase VP1. The latter change, together with Ala270Thr change

in VP2, proved to be associated with viral attenuation *in vivo*. These results identify genome sequences that are important for IBDV evolution in response to selection pressures. Such information will help tailor better strategies for controlling IBDV infection in chickens.

**Keywords: IBDV, chicken B cells, evolution, 7DMA, viral diversity, mutation frequency, passages**

## INTRODUCTION

Infectious bursal disease (IBD) is caused by IBD virus (IBDV) and was observed for the first time in Delaware (United States) in 1957 (Cosgrove, 1962). This highly contagious disease affects young chickens, representing a serious threat to the poultry industry worldwide. After infection by the oral route, IBDV replicates in several lymphoid organs; the Bursa of Fabricius (BF) (a bird-specific primary lymphoid organ where the maturation of avian B cells occurs) is IBDV main target. Once in the BF, IBDV replicates actively in immature IgM<sup>+</sup> B cells, causing bursal atrophy, immunosuppression and sometimes death (Dey et al., 2019).

Infectious bursal disease virus belongs to the family *Birnaviridae*, genus *Avibirnavirus*, and is a naked and bisegmented double-stranded RNA virus. Segment A (3.2 kbp) encodes two open reading frames (ORFs), which are partially overlapping. The first ORF encodes the 21 kDa non-structural viral protein 5 (VP5), while the second one codes for a 110 kDa polyprotein which is further cleaved by autoproteolysis to yield mature VP2 (capsid protein, 42 kDa), VP4 (protease, 28 kDa) and VP3 (scaffold protein, 32 kDa). The smaller segment B (2.8 kbp) encodes VP1 (97 kDa), the RNA-dependent RNA polymerase, RdRp (Dey et al., 2019; Etteradossi and Saif, 2020). VP2 contains a hypervariable region, hVP2, which carries the immunogenic determinants and spans from amino acid position 206 to 350 (Bayliss et al., 1990; Coulibaly et al., 2005; Dey et al., 2019). Mutations in hVP2 positions 253, 279, 284 and 330 have been related with both adaptation to avian and mammalian cell culture and viral attenuation in chickens of pathogenic field strains (Lim et al., 1999; van Loon et al., 2002; Noor et al., 2014).

Based on virus neutralization assays, IBDV strains are classified as belonging to serotype 1 or 2. Serotype 1 viruses can infect chickens, guinea fowls, ducks, quails, turkeys, pheasants and ostriches (Dey et al., 2019; Etteradossi and Saif, 2020). However, clinical forms of IBD, observed after infection by serotype 1 viruses, have only been reported in young chickens (3–8 weeks of age). Although infections by serotype 2 viruses have been demonstrated in chickens, ducks, fowls and turkeys (McFerran et al., 1980), these viruses are non-pathogenic. Depending on their pathogenicity in chickens, viruses from serotype 1 are further classified as classical virulent (cvIBDV), very virulent (vvIBDV) or subclinical (antigenic variants). IBD was effectively controlled until the 1980s by vaccines developed against classical strains. However, the emergence of vvIBDV in Europe (Chettle et al., 1989) and antigenic variants in the United States (Jackwood and Saif, 1987) during the 80s resulted in economic losses and high mortality in chickens. Since then, vvIBDV have spread and been reported in many parts of

the world (Dey et al., 2019). Questions about unique genetic mutations involved in the evolution and expansion of vvIBDV remain open. Attenuated vaccines currently used to protect from IBD elicit a more robust immune response when compared to inactivated vaccines, but they convey the risk of reversion toward higher virulence (Olesen et al., 2018; Dey et al., 2019; Etteradossi and Saif, 2020). Thus, a better knowledge of the evolution of IBDV as well as new strategies in the development of safer and more stable vaccines are required to improve the control of emerging IBDV strains.

The relatively low intrinsic fidelity of RdRp is responsible in large part for the high mutation rates in RNA viruses, which appear to be the highest of all organisms (Borderia et al., 2016). These high mutation rates contribute to the generation of complex and dynamic mutant spectra, which facilitate virus adaptation and evolution in response to selection pressures. However, there is a maximum error rate, also called error threshold, above which genetic information can no longer be maintained, resulting in an error catastrophe and an abortive infection (Eigen, 2002; Domingo and Perales, 2019). Lethal mutagenesis is a particular case of error catastrophe. In this situation, during viral genome replication, mutagenic nucleoside analogs are incorporated by viral polymerases into the nascent strand of RNA, resulting in the accumulation of mutations above the error threshold, which is lethal for the virus. This concept explains the interest of nucleoside analogs as antiviral treatments (Crotty et al., 2000). However, the use of moderately toxic nucleoside analog concentrations can select resistant mutants. This resistant phenotype is often explained by mutations in the viral polymerase gene that alter the polymerase intrinsic fidelity, resulting in an expansion (low fidelity) or reduction (high fidelity) of the viral population diversity (Borderia et al., 2016). The study of those fidelity mutants has highlighted the role of mutant spectrum on the pathogenesis, adaptability to new environments and viral evolution of several RNA viruses. Fidelity mutants were for instance reported for poliovirus (Pfeiffer and Kirkegaard, 2003), Coxsackie virus B3 (Levi et al., 2010; Gnadig et al., 2012), foot-and-mouth disease virus (Zeng et al., 2013), chikungunya (Coffey and Vignuzzi, 2010), influenza A (Cheung et al., 2014) or West Nile (Van Slyke et al., 2015) viruses.

In the present study, two strains of IBDV produced from cloned DNA in a reverse genetics system (Cubas-Gaona et al., 2020) were used: one based on a non-passaged (p0), cell-culture adapted, attenuated, vaccine-related and classical strain (rCu-1-p0), and a second one based on a non-passaged, non-cell-culture adapted and very virulent strain (rvv-p0). rCu-1-p0 was serially passaged in DF-1 cells, chicken bursal cells (hereafter referred as chicken B cells), and chickens while rvv-p0 was exclusively passaged using chicken B cells to address four

questions: (i) whether serial passaging of a homogeneous rrvv-p0 virus population would select mutations previously observed upon wild-type heterogeneous vvIBDV adaptation to avian and mammalian cell cultures, (ii) whether serial passaging of homogeneous rCu-1-p0 virus population would select mutations associated to a reversion toward virulence of some heterogeneous live-attenuated vaccines, (iii) whether serial passaging in the presence of the adenosine analog 7-deaza-2'-C-methyladenosine (7DMA) would generate resistant mutants in one or both homogeneous virus populations, and (iv) whether potential resistant mutants would show an attenuated phenotype *in vivo*.

Viral stocks produced before and after serial passages were deep-sequenced to explore the composition of their viral populations and provide insights in the evolutionary trajectories, genetic variability and host adaptability of IBDV.

## MATERIALS AND METHODS

### Cell and Viruses

The chicken fibroblast DF-1 cell line (ATCC CRL-12203) was grown in Dubelcco's modified minimal essential medium (DMEM) (reference 61965-023, Thermo Fisher) supplemented with 10% fetal bovine serum (FBS), penicillin (200 IU/mL), streptomycin (0.2 mg/mL), fungizone (2 µg/mL) and maintained at 39 °C in a humidified 5% CO<sub>2</sub> incubator.

The rescue of recombinant viruses rCu-1-p0 and rrvv-p0 has been described recently (Cubas-Gaona et al., 2020). Briefly, DF-1 cells were transfected with recombinant expression vectors prACu-1 and prBCu-1 for rCu-1-p0 recovery or prAvv and prBvv for rrvv-p0 recovery. After 72 h, cellular material was transferred onto B cells. At 48 h post transfer, the supernatants were recovered, aliquoted and titrated on B cells. The viral sequences used for rrvv rescue are available in Genbank with the accession number MG489893 (for segment A) and MG489892 (for segment B). The viral sequences used for rCu-1 rescue are presented in **Supplementary Table 1**. The classical virulent strain rCu-1 presents more than 99% identity for both segments A and B with D78 and Cu-1 M, two live-attenuated vaccines used in Europe.

### Isolation of Primary Chickens Bursal Cells

All animal trials were conducted in an animal facility approved for animal experiments (n° C-22-745-1) and were approved by ANSES Ploufragan local committee for animal welfare; chickens were raised and humanely euthanized in agreement with EU directive number 2010/63/UE.

For experimental passages and viral titrations, BF were aseptically collected from four to ten week-old specific-pathogen-free (SPF) White Leghorns chickens (ANSES, Ploufragan, France) and were processed as previously described (Soubies et al., 2018). Bursal cells were maintained in lymphocyte culture medium at 40 °C in a humidified 5% CO<sub>2</sub> incubator. This medium was prepared using Iscove's modified Dulbecco's Medium (IMDM) with L-glutamine and HEPES (reference 21980-032, Gibco, Thermo Fisher) supplemented with 8% FBS, 2% SPF chicken serum (ANSES, Ploufragan, France),

1X insulin transferrin selenium (reference 41400-045, Gibco, Thermo Fisher), 50 µM beta-mercaptoethanol, 1 µg/mL Phorbol 12-myristate 13-acetate (PMA, reference tlr1-pma, Invivogen), penicillin (200 IU/mL), streptomycin (0.2 mg/mL) and fungizone (2 µg/mL). PMA was reconstituted as previously described (Soubies et al., 2018). Bursal cells were diluted into phosphate-buffered saline (PBS) containing 0.1% (m/v) erythrosin B (reference 200964, Sigma-Aldrich) and counted in a Neubauer chamber to estimate cell viability and numbers after isolation.

### Virus Titration by Immunocytochemistry (ICC)

Ten-fold serial dilutions of viral stocks and of supernatants from cells in IMDM were distributed into 96-well U bottom plates (50 µL/well, eight replicates per viral sample). Freshly prepared chicken B cells in lymphocyte culture medium (10<sup>6</sup> cells in 150 µL/well) were added in each well and incubated at 40 °C for 48 h in a humidified 5% CO<sub>2</sub> incubator. Forty-eight hours post-infection (h.p.i.), the cells were washed with PBS and fixed with ethanol and acetone solution (1:1 ratio) at -20°C for at least 30 min. After removal of the fixation solution, the plates were air-dried under a chemical hood and processed immediately or stored at -20°C until further processing. The plates were subjected to ICC as previously described (Soubies et al., 2018). Viral titers expressed as TCID<sub>50</sub>/mL were determined using Reed and Muench formula (Reed and Muench, 1938).

### Experimental Passages in Cells and in Chickens

Either 5 × 10<sup>6</sup> DF-1 or 5 × 10<sup>7</sup> chicken B cells were seeded in 10 mL of their respective complete medium, as indicated above, on 25 cm<sup>2</sup> flasks. Chicken B cells were promptly subjected to infection after isolation, while DF-1 cells were seeded 5 h before infection. DF-1 and chicken B cells were infected in 1 mL medium at a multiplicity of infection (MOI) of 0.1 and 0.01, respectively. After 1 h of viral adsorption in 1 mL medium with frequent rocking, the inoculum was removed. Fresh medium with or without 7-deaza-2'-C-methyladenosine (7DMA, reference ND08351, Carbosynth) at 2.5 µM for rCu-1 and 4 µM for rrvv was added. The optimal non-toxic concentration of 7DMA was determined following the recommendations previously described (Beaucourt et al., 2011). After 24 h (chicken B cells) or 48 h (DF-1 cells), cells debris were removed by centrifugation and the supernatants were harvested and aliquoted before freezing at -70°C. One aliquot was titrated by ICC, as indicated above, to determine the required inoculum dilution for the next passage. rCu-1-p0 was passaged twelve times in parallel in chicken B cells and DF-1 cells (MOI of 0.01 and 0.1 at each passage, respectively). rrvv-p0 was passaged twelve times at a constant MOI of 0.01 in chicken B cells only, since this strain does not replicate in DF-1 cells. Three parallel and independent stocks (called R1, R2 and R3, respectively) were produced for each condition and passage.

Serial passages of rCu-1-p0 in chickens were approved by ANSES ethical committee, registered at the national level under number C2EA-016/ComEth ANSES/ENVA/UPEC and authorized by French Ministry for higher education and research

under permit number APAFiS#2494-201512021054584v1. For each passage, 5 five-to-eight-week-old SPF White Leghorns chickens (ANSES, Ploufragan, France) were housed in a single negative-pressure filtered-air isolators and infected by the intranasal route with rCu-1 at  $10^5$  TCID<sub>50</sub>/animal in 0.1 mL PBS containing penicillin (200 IU/mL), streptomycin (0.2 mg/mL) and fungizone (2 µg/mL). At 4 days post-inoculation (d.p.i.), the five chickens were humanely euthanatized and BFs were collected aseptically, pooled and processed to prepare the viral stock for the next passage (see below). BFs were pooled in order to avoid creating a bias by selecting determined viral populations. After each passage, viral stock was titrated by ICC to adjust the dilution of the inoculum for the next passage and to infect at  $10^5$  TCID<sub>50</sub> per animal. A total of five passages in chickens were performed, similarly, to what is required by the European Pharmacopoeia to assess virus stability in the licensing process of IBDV live-attenuated vaccine-candidates. The codification for the different viral stocks is shown in **Supplementary Table M1**. A graphical overview of the different passaging procedures is presented in **Figure 1A**.

## Preparation of Viral Stocks From Bursae of Fabricius

Tissue homogenization was performed using either Ultra-Turrax T25 basic IKA or TissueLyser (Qiagen) homogenizers to process pool or individual BFs, respectively. All steps were carried out on ice. Briefly, bursae were weighed and cut into small segments. One milliliter of PBS was then added per gram of bursa before homogenizing. 1,1,1,2,3,4,4,5,5,5-Decafluoropentane (reference 94884, Sigma) was added to the tissue suspension (1:1 ratio) and an additional homogenization step was carried out. For Ultra-Turrax homogenizer procedure, the tissue suspension was spun at 1260 g for 30 min and supernatants were recovered. For TissueLyser homogenizer, tissue suspensions were shook at high-speed with a stainless steel bead for 3 min at 30 Hz, followed by centrifugation at 4000 g for 30 min. Supernatants were collected and stored at  $-70^{\circ}\text{C}$ .

## Purification and Concentration of Viral Stocks

To purify rCu-1-p5/ch viral stock, the resin Cpto™Core 700 (reference 17548101, GE Healthcare), which retains molecules below 700 kDa and thus not viral capsids, was used as previously described (James et al., 2016). Three milliliters of viral stock were centrifuged for 10 min at 12000 g and supernatant was recovered and filtered through a 0.22 µm filter (Hall et al., 2014). The resin was washed 3 times with PBS, with shaking (5 min at low speed) followed by centrifugation (3 min at 800 g) in each washing step. Then, three sequential in-slurry purifications as previously described (James et al., 2016) were carried out in 15 mL tubes, using a ratio of five volumes of viral stock for each volume of resin. In each purification step, the mix was homogenized at low speed for 45 min on a rotator holder then centrifuged for 10 min at 800 g; supernatant was recovered and transferred into a new 15 mL tube containing resin. After the third purification, supernatants were subjected to concentration (see below). Viral

stocks prepared from chicken B cells and DF-1 cells used for passage 12 of rCu-1 and from chicken B cells used for passage 12 of rvv (see above) were directly concentrated.

Supernatants were concentrated up to around 200 µL in Pierce™ Protein Concentrator PES, 100K MWCO (reference 88524, Thermo Scientific) for 30 min at 3600 g and then stored at  $-70^{\circ}\text{C}$ . All samples were then subjected to RNA extraction.

## RNA Extraction, Viral Genome RT-PCR, Gel Electrophoresis and Purification

One hundred and forty microliters from different viral stocks were RNA-extracted using the QIAamp viral RNA mini kit (reference 52904, Qiagen) following the manufacturer's instructions. However, linear acrylamide (reference AM9520, Thermo Fisher) at 0.025 mg/mL was used instead of carrier RNA. RNA concentration was determined by using Qubit RNA HS assay kit (Invitrogen, Q32852) in the Qubit®2.0 Fluorometer.

The isolation of viral RNA from cloacal swabs was carried out using the NucleoMag®VET kit (reference 744200, Macherey Nagel) in the KingFisher®Flex system (reference 744950, Macherey Nagel), according to the manufacturer's instructions. The obtained viral dsRNA was denatured in presence of DMSO at  $94^{\circ}\text{C}$  for 4 min, then chilled on ice for 2 min. qRT-PCR was subsequently performed using QuantiTect Probe RT-PCR kit (reference 204443, Qiagen) according to the manufacturer's protocol. Reactions were performed as follow: 30 min at  $50^{\circ}\text{C}$ , 15 min at  $95^{\circ}\text{C}$ , 40 cycles each comprising 15 s at  $94^{\circ}\text{C}$  and 1 min  $60^{\circ}\text{C}$ . The primers and probe used, which target a portion of VP3 coding region (CDR), were previously described (Escaffre et al., 2010).

Infectious bursal disease virus genome from individual BF or viral inocula used to infect chickens were reverse-transcribed into cDNA by Maxima H minus Reverse Transcriptase (reference EP0752, Thermo Fisher) according to the manufacturer's protocol. The reaction was incubated at  $50^{\circ}\text{C}$  for 30 min and heated at  $85^{\circ}\text{C}$  for 5 min to inactivate the enzyme. cDNA was subjected for partial or full-segment PCR amplification with Phusion Hot Start II DNA polymerase (reference F549S, Thermo Fisher) following the manufacturer's instructions. Reactions were performed as follow: 30 s at  $98^{\circ}\text{C}$ , 35 cycles each comprising 10 s at  $98^{\circ}\text{C}$ , 15 s at  $T_m$ , t at  $72^{\circ}\text{C}$  and a final step at  $72^{\circ}\text{C}$  for 5 min. Primer sets used during reverse-transcription and PCR, together with  $T_m$  and t for each PCR are presented in **Supplementary Table 2**. The segments A and B from each sample were separated by 1% agarose-gel electrophoresis, eluted in ultra-pure water by Gel and PCR clean up kit (reference 740609, Macherey Nagel). DNA concentrations were measured by using Qubit dsDNA HS assay kit (Invitrogen, Q32854) in the Qubit®2.0 Fluorometer.

## Study of Pathogenicity in Chickens

Pathogenicity assessment in SPF chickens was approved by ANSES ethical committee, registered at the national level under number C2EA-016/ComEth ANSES/ENVA/UPEC and authorized by French Ministry for higher education and research under permit number APAFiS#4945-20 16041316546318 v6. Eighty, three-week-old SPF White Leghorns chickens

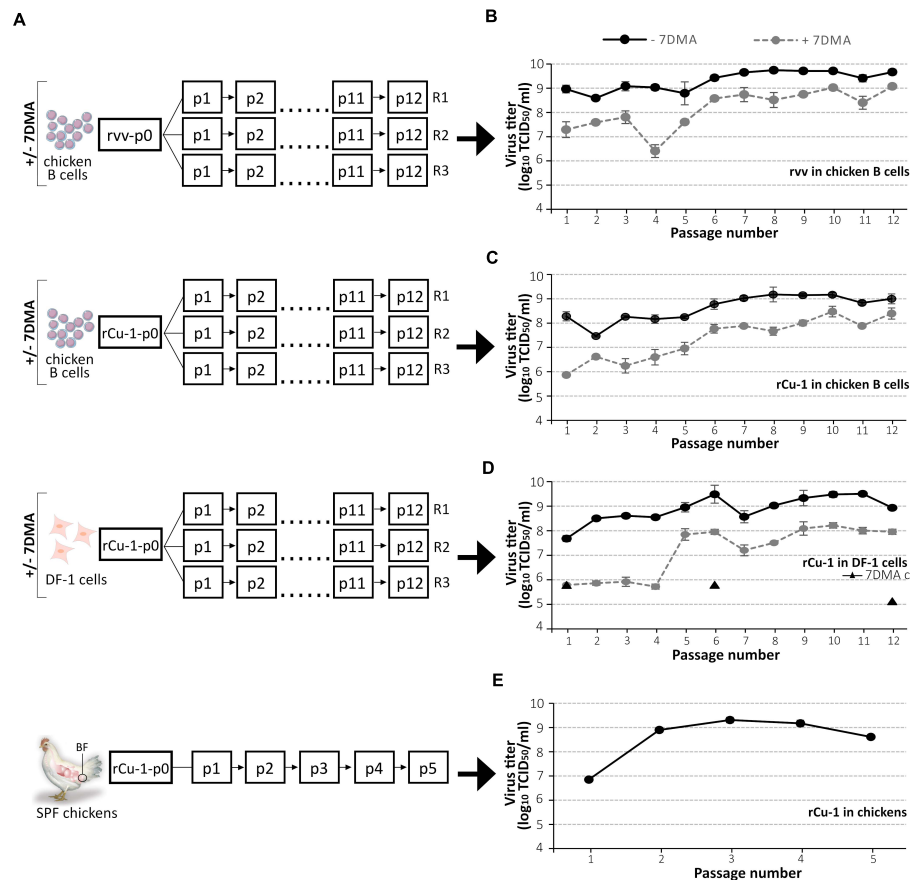


**FIGURE 1 |** IBDV titer evolution during passages *in vitro*, *ex vivo*, and *in vivo*. **(A)** Layout of the serial passage strategy. For *in vitro* passages, a constant multiplicity of infection (MOI) of 0.01 and 0.1 was used in chicken B cells and DF-1 cells, respectively. For *ex vivo* and *in vitro* experiments, in chicken B cells and DF-1 cells, respectively, viral stocks from each passage were titrated in chicken B cells to adjust the infecting dose for the next passage. For *in vivo* experiments, five specific pathogen-free (SPF) chickens were inoculated with  $10^5$  TCID<sub>50</sub>/animal in 0.1 mL PBS of rCu-1-p0 by the intranasal route. The five Bursae of Fabricius (BF) were collected 4 days post-inoculation, pooled and titrated in chicken B cells to adjust the infecting dose for the next passage. For each condition, each replicate of the final passage was sequenced by NGS (RNA deep-sequencing). Virus progeny titers after each of the 12 passages in cells in the presence or the absence of 7DMA treatment **(B–D)** or rCu-1 progeny titers after each of the 5 passages in chickens **(E)**. 7DMA c (triangle): control for constant activity of the drug 7DMA; DF-1 were infected with rCu-1-p0 in the presence of 7DMA in parallel of p1, p6, and p12. The anatomical position of the BF is indicated by a circle. p: number of passage; p0: inoculum; R: replicate. Bars indicate means  $\pm$  SD based on three replicates for each passage and condition.

(ANSES, Ploufragan, France) were distributed into 4 groups of 20 birds, named P1, P2, P3, and P4, of similar weight and sex, housed in separate negative-pressure filtered-air isolators. Three days before inoculation, blood samples were collected from 27 chickens in order to confirm their seronegativity for IBDV using a viral neutralization assay as previously described (Etteradossi et al., 1992). Viral inocula were prepared by diluting viral stocks in a diluent made of PBS with penicillin (200 IU/mL), streptomycin (0.2 mg/mL) and fungizone (2  $\mu$ g/mL). Chickens from groups P1, P2 and P3 were inoculated by the intranasal route with rVv-p0, rVv-p12 or rVv-p12/7DMA, respectively, at  $10^6$  TCID<sub>50</sub> in 0.1 mL per animal. Chickens from group P4 were mock-inoculated with diluent.

Mortality rates were followed throughout the animal experiment, which lasted for 21 days. Clinical signs were measured daily based on the symptomatic index previously

developed which ranges from 0, “lack of signs” to 3, “typical severe IBD signs with prostration or death,” which is the ethical endpoint (Le Nouen et al., 2012). Cloacal swabs were collected in 1 mL PBS at 0–4, 7, 14, and 21 d.p.i. to measure viral shedding by qRT-PCR (see section 2.7).

Ten randomly chosen chickens were blood sampled at the venous occipital sinus using commercial EDTA coated blood collection devices (Monovette®, Sarstedt) at 2 and 21 d.p.i. to perform white blood cell counting as described in 2.9.

At 4 d.p.i. and 21 d.p.i., five chickens per group and all remaining chickens, respectively, were weighed, humanely euthanized, necropsied and their spleens and BFs were collected and weighed for calculating the spleen-to-body-weight ratio [s/B] and the bursa-to-body-weight ratio [b/B], respectively. Then, the bursae harvested at 4 d.p.i. were processed for virological analyses as indicated above (see section 2.5) for virus titration (see section 2.3).

## Flow Cytometry

The protocol for chicken white blood cells counting was performed according to Seliger et al. (2012). All blood samples were processed within 4 h after blood collection. Briefly, EDTA-blood samples were diluted in PBS with 1% FBS, mixed with the labeled antibody mixture and incubated for 30 min with agitation, at room temperature and in the dark. The antibodies and fluorochrome conjugates used in this study were similar to those used by Seliger et al. (2012) and they are listed in **Supplementary Table 3**. The gating strategy is showed in **Supplementary Figure 1**. After incubation, approximately  $5 \times 10^4$  Precision Count Beads (reference BLE424902, BioLegend) prepared in PBS-FBS were added to each sample to determine the absolute counts of cells. In the last step, formaldehyde (1% final concentration per sample) was added and the samples were incubated for 15 min with frequent agitation at room temperature and in the dark to inactivate the virus. Samples were analyzed on a FC500 MPL flow cytometer (Beckman Coulter).

## Sequencing of Genomic Segments by Next Generation Sequencing (NGS)

To quantify IBDV evolution, RNA molecules were extracted from rvv-p0 and rCu-1-p0, all stocks obtained after passage 12 in chicken B cells and DF-1 cells and after passage 5 in chickens. These RNAs were then analyzed by a next generation sequencing (NGS) approach.

For RNA sequencing, NGS was performed on the RNA extract after rRNA depletion with the Low Input Ribominus Kit (Ambion), as described by the manufacturer. A RNA library was obtained using Ion total-Seq Kit v2 (Life Technologies) according to the manufacturer's recommendations and was then sequenced with using Ion Torrent Proton technology.

For DNA sequencing, PCR fragments were purified and quantified as described above. Illumina libraries were prepared with the Nextera XT kit (Illumina) according to the supplier's recommendation. Paired-end sequencing (150 nt long) was performed on an Illumina NovaSeq 6000.

All sequencing reads were processed to remove low quality or artefactual reads followed by bioinformatics analysis as previously described (Abed et al., 2018). The data were deposited in the BioSample database at NCBI under accession numbers from SAMN14642839 to SAMN14642909.

An in-house bioinformatics pipeline, VVV (Flageul et al., 2021) was used to identify single nucleotide variation (SNV) frequencies above an empirically determined cut-off frequency of 7% to exclude the errors introduced by reverse-transcription, PCR and sequencing. Sequences of the PCR primers (**Supplementary Table 2**) as well as nucleotide substitutions in homopolymer regions and insertions and deletions were removed from the analysis (Song et al., 2017). The total variants which passed these criteria were used to calculate the nucleotide diversity ( $\pi$ ), which allows to measure viral sequence diversity without bias due to the depth of sequencing. At the locus  $l$ ,  $n_i$  (copies of the allele  $i$  in the A, T, C, G set) was calculated as  $n_i = p_i/N$  and  $n_j = 1 - n_i$  where  $N$  is the read depth at the locus  $l$  and the frequency of each nucleotide  $i$  was given by  $p_i$ .

Then, the proportion of pairwise differences between alleles can be denoted  $DI$  (Zhao and Illingworth, 2019):

$$DI = \frac{\sum_{i \neq j} n_i n_j}{\frac{1}{2} N(N-1)} = \frac{N(N-1) - \sum_i n_i(n_i-1)}{N(N-1)}$$

Therefore, the statistic  $\pi$  was calculated for all covered positions in each genomic segment ( $L$ ) as,

$$\pi = \sum_{l=1}^L DI/L$$

To render a more user-friendly number,  $\pi$  values were multiplied by 10 000.

## Prediction of RNA Secondary Structures of rvv-p0, rvv-p12, rCu-1-p0, and rCu-1-p12/B and Detection of Mutations Present in Other Naturally Occurring IBDV Strains

RNA secondary structures were predicted using mFold\_util version 4.7 online tool (Zuker, 2003). Complete or nearly complete sequences of segments A and B of IBDV were downloaded from Genbank database<sup>1</sup>. Sequences with too many ambiguous nucleotide positions were removed. Amino acid sequences for each viral protein were aligned using MAFFT program. After alignment, sequences of vaccine or laboratory-derived strains were excluded from the analysis.

## Statistical Analysis

Statistical analyses were performed using R version 3.6.1 and RStudio Version 1.2.5019. Differences in mortality were analyzed by logistic regression using the "glm" function from the package "stats" version 3.6.1., associated with a binomial link. All other quantitative parameters were analyzed using Kruskal-Wallis test followed by Fisher's least significant difference test with Holm adjustment method for multiple comparisons using the "kruskal" function from the package "Agricolae" version 1.3–2.

## RESULTS

### Viral Titer Evolution During Passages in Cells and Chickens

To help to understand the different molecular mechanisms that drive viral adaptation and evolution in different environments, rCu-1-p0 and rvv-p0 were passaged 12 times in the absence and presence of 7DMA with a defined MOI in chicken B cells. Additionally, the genetic stability of rCu-1-p0 genome upon passages *ex vivo* in chicken B cells was compared to its passages *in vitro* in DF-1 cells and *in vivo* in chickens. As rvv is not adapted to cell culture in DF1, this virus was not passaged on this cell line; this virus was also not passaged in chickens.

<sup>1</sup><https://www.ncbi.nlm.nih.gov/genbank/>

**Figure 1A** shows the layout followed during the different passages. In the absence of 7DMA and in DF-1 and chicken B cells, rvv and rCu-1 titers showed little variation, about 0.2–0.7 log<sub>10</sub> (TCID<sub>50</sub>/mL), between one passage and the next (**Figures 1B–D**). Passaging of rCu-1 in chickens resulted in an increase of around 2 log<sub>10</sub> (TCID<sub>50</sub>/mL) between p1 and p2; virus yield remained similar after p2 (**Figure 1E**). No clinical sign was observed during the *in vivo* passages of rCu-1 although bursae were collected 4 days post-infection, a moment when clinical signs usually reach their maximum for pathogenic IBDV strains.

During the first passage, 7DMA treatment provoked, in agreement with preliminary tests, a mean reduction of rvv titer of 1.7 log<sub>10</sub> (TCID<sub>50</sub>/mL) in chicken B cells and, in rCu-1, a mean reduction of 2.4 and 1.9 log<sub>10</sub> (TCID<sub>50</sub>/mL) in chicken B cells and DF-1 cells, respectively. In presence of 7DMA, titers were notably lower in DF1 cells in early passages (1–4) (around 6 log<sub>10</sub> (TCID<sub>50</sub>/ml)) compared to those of the same viruses passaged in the absence of 7DMA (around 8.5 log<sub>10</sub> (TCID<sub>50</sub>/ml)). However, after passage 4 and in presence of 7DMA, these increased to around 7.8 log<sub>10</sub> (TCID<sub>50</sub>/ml), which was within 1 to 1.5 log<sub>10</sub> (TCID<sub>50</sub>/ml) of titers obtained for the same viruses passaged in the absence of 7DMA (**Figure 1D**). A similar effect in passages 1–5 was observed in chicken B cells for both rCu-1 and rvv; however, this was less marked (**Figures 1B,C**).

As a control for 7DMA activity, DF-1 were infected with rCu-1-p0 in the presence of 7DMA in parallel of passages 1, 6 and 12. The resulting viral titers, of 5.8 log<sub>10</sub> (TCID<sub>50</sub>/mL) in p1, 5.8 log<sub>10</sub> (TCID<sub>50</sub>/mL) in p6 and 5.1 log<sub>10</sub> (TCID<sub>50</sub>/mL) in p12, similar to those observed in initial passages upon 7DMA treatment, showed constant activity of the drug 7DMA (**Figure 1D**, triangle).

Collectively, data indicated an increased resistance of the IBDV strains passaged in the presence of 7DMA, possibly associated to some event of mutation after passage 4 or 5.

## Variant Frequency, Mutation Frequency and Nucleotide Diversity ( $\pi$ ) of rvv and rCu-1 After Passages

To quantify IBDV evolution, RNA molecules were extracted from rvv-p0 and rCu-1-p0, all stocks obtained after passage 12 in chicken B cells and DF-1 cells and after passage 5 in chickens. These RNAs were then analyzed by NGS. Assembled sequences were further analyzed to calculate the variant frequency, mutation frequency and nucleotide diversity ( $\pi$ ). The frequency and distribution of SNVs are presented in **Tables 1–3**. For clarity sake, only mutation frequency and nucleotide diversity values are in detail below.

### rvv in Chicken B Cells

No SNV was observed in rvv-p0 segment A nor B viral RNA population (**Table 1**) compared to the consensus sequence of the plasmid inserts sequences of rvv.

### Analysis of segment A of rvv-p12 and rvv-p12/7DMA

For rvv-p12, mutation frequencies of 14.8, 15.2, and 4.3 substitutions per 10 000 nucleotides (sub/10<sup>4</sup> nt) were observed for VP5, VP2 and VP4, respectively.

For rvv-p12/7DMA, mutation frequency in VP2 (13 sub/10<sup>4</sup> nt) was similar to that in rvv-p12, while this frequency was 3 times higher in VP4 CDR in rvv-p12/7DMA (13 sub/10<sup>4</sup> nt) compared to that in rvv-p12.

In segment A, the mutation frequency as well as the nucleotide diversity, determined through the statistic  $\pi$  were comparable for both viral stocks (**Table 1**).

### Analysis of segment B of rvv-p12 and rvv-p12/7DMA

For rvv-p12, 3 SNVs were found (**Table 1**), located in the 3'UTR in one single nucleotide position.

For rvv-p12/7DMA, 11 SNVs were found (**Table 1**), all of them located in VP1 ORF in 9 nucleotide positions, with a mutation frequency of 13.9 sub/10<sup>4</sup> nt.

The mutation frequency increased from 3.5 sub/10<sup>4</sup> nt in rvv-p12 to 13 sub/10<sup>4</sup> nt in rvv-p12/7DMA. Unlike segment A, in segment B, the nucleotide diversity increased 3 times in rvv-p12/7DMA ( $3 \times 10^{-4}$ ) compared with rvv-p12 ( $1 \times 10^{-4}$ , **Table 1**).

### rCu-1 in Chicken B Cells, DF-1 and Chickens

rCu-1-p0 harbored a single SNV in segment A (in the region belonging to both VP5 ORF and VP2 CDR) and another one in segment B, with frequencies below 10% (**Table 2**).

After 12 passages in chicken B cells and DF-1 as well as after 5 passages in chickens of rCu-1-p0, several SNVs were distributed throughout the genome in coding as well as non-coding regions in both segments regardless of the condition used.

### Analysis of segment A from rCu-1-p12/B and rCu-1-p12/B/7DMA

In rCu-1-p12/B, mutations frequencies of 7.6, 8.7, 32, and 26 sub/10<sup>4</sup> nt were observed for VP5, VP2, VP4 and VP3, respectively. In rCu-1-p12/B/7DMA, mutation frequencies of 15.2, 6.5, 27.3, and 21.6 sub/10<sup>4</sup> nt were observed for VP5, VP2, VP4 and VP3, respectively. In segment A, the mutation frequency as well as the nucleotide diversity were comparable in both viral stocks (**Table 2**).

### Analysis of segment B from rCu-1-p12/B and rCu-1-p12/B/7DMA

In rCu-1-p12/B, a mutation frequency of 5 sub/10<sup>4</sup> nt was observed in VP1 ORF. This frequency increased 3 times rCu-1-p12/B/7DMA.

For segment B, in rCu-1-p12/B, a mutation frequency of 4.7 sub/10<sup>4</sup> nt and a nucleotide diversity of  $0.7 \times 10^{-4}$  were observed. In rCu-1-p12/B/7DMA, the mutation frequency and the nucleotide diversity increased 3 and 4.1 times, respectively, with respect to rCu-1-p12/B.

### Analysis of segment A from rCu-1-p12/DF-1 and rCu-1-p12/DF-1/7DMA

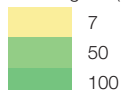
In rCu-1-p12/DF-1, mutation frequencies of 7.6, 8.7, 4.6, and 17.3 sub/10<sup>4</sup> nt were observed for VP5, VP2, VP4 and VP3, respectively (**Table 3**).

In rCu-1-p12/DF-1/7DMA, comparable mutation frequencies with respect to rCu-1-p12/DF-1 were observed in VP5, VP3

**TABLE 1** | Analysis of variant frequencies and genetic variation in IBDV genome of rvv-p0, rvv-p12, and rvv-p12/7DMA characterized by RNA deep-sequencing.

IBDV segment	Genomic region	nt position	nt substitution <sup>a</sup>	aa substitution <sup>b</sup>	rvv-p0	rvv-p12			rvv-p12/7DMA			
						R1	R2	R3	R1	R2	R3	
A	5'UTR	50	<b>A:G</b>						11%			
		53	<b>C:U</b>							9%		
		54	<b>C:U</b>								15%	
	VP5	90	<b>CUA:CUG</b>	Leu2Leu					8%			
		103	<b>AGU:GGU</b>	Ser7Gly					8%			
	<i>VP5 Mutation frequency (sub/10<sup>4</sup> nt)</i>					0	14.8			0		
	VP2	779	<b>UCA:ACA</b>	Ser217Thr					19%			
		795	<b>GCA:GUA</b>	Ala222Val		13%	10%	11%				
		938	<b>GCG:ACG</b>	Ala270Thr					88%	81%	47%	
		939	<b>GCG:GAG</b>	Ala270Glu		81%	71%	89%				
		941	<b>GUA:AUA</b>	Val271Ile							21%	
		1021	<b>CCA:CCG</b>	Pro297Pro							9%	
		1313	<b>AUG:GUG</b>	Met395Val							10%	
	<i>VP2 Mutation frequency (sub/10<sup>4</sup> nt)</i>					0	15.2			13		
	VP4	2351	<b>UAC:CAC</b>	Tyr741His		30%			32%	12%	9%	
	<i>VP4 Mutation frequency (sub/10<sup>4</sup> nt)</i>					0	4.3			13		
	<i>Mean coverage</i>					226	107	346	237	292	119	34
	<i>Total number of SNVs</i>					0		10			12	
	<i>Mean number of SNVs<sup>c</sup></i>					0		3.3			4	
	<i>Mean number of Non-Synonymous-SNVs</i>					0		3			2.7	
<i>Mean number of Synonymous-SNVs</i>					0		0.3			0.3		
<i>Mutation frequency (sub/10<sup>4</sup> nt)<sup>d</sup></i>					0		10.2			12.3		
<i>Nucleotide diversity, π (× 10<sup>-4</sup>)</i>					0		2.6			3.2		
B	VP1	584	<b>AAC:AGC</b>	Asn158Ser							13%	
		597	<b>AAA:AAC</b>	Lys162Asn							14%	
		1096	<b>ACA:GCA</b>	Thr329Ala					99%	96%	73%	
		1116	<b>CGU:CGC</b>	Arg335Arg							14%	
		1440	<b>GAU:GAC</b>	Asp443Asp							8%	
		2112	<b>UCA:UCG</b>	Ser667Ser							8%	
		2280	<b>GGU:GGC</b>	Gly723Gly					13%			
		2673	<b>GGG:GGA</b>	Gly854Gly							23%	
		2718	<b>AAA:AAG</b>	Lys869Lys							27%	
	<i>VP1 Mutation frequency (sub/10<sup>4</sup> nt)</i>					0	0			13.9		
	3'UTR	2764	<b>C:U</b>			83%	80%	84%				
	<i>Mean coverage</i>					221	95	273	217	467	179	38
	<i>Total number of SNVs</i>					0		3			11	
	<i>Mean number of SNVs<sup>c</sup></i>					0		1			3.7	
<i>Mean number of Non-Synonymous-SNVs</i>					0		0			1.7		
<i>Mean number of Synonymous-SNVs</i>					0		0			2		
<i>Mutation frequency (sub/10<sup>4</sup> nt)<sup>d</sup></i>					0		3.5			13		
<i>Nucleotide diversity, π (× 10<sup>-4</sup>)</i>					0		1			3		

Color legend (Frequency in %)



<sup>a</sup>Nucleotide (nt) substitution column show in bold the nt replaced (on the left) by the new one (on the right) after passages in the corresponding untranslated (UTR) or coding regions. For coding regions, other nucleotides from the same codon are displayed.

<sup>b</sup>Amino acid (aa) substitution indicated in VP5 ORF, the polyprotein or VP1 ORF.

<sup>c</sup>Mean number of SNV (single nucleotide variant) was obtained by dividing the total number of SNVs by the number of replicates.

<sup>d</sup>To obtain mutation frequency per 10 000 nucleotides (nt) sequenced, mean number of SNVs was divided by the total genome length (3260 nt for segment A or 2827 nt for segment B) and then multiplied by 10 000 nt to display a more user-friendly number. Sub: substitutions.

R (replicate). Variant frequency is color-coded from yellow (frequency of 7%) to green (frequency of 100%).

**TABLE 2 |** Analysis of variant frequencies and genetic variation in IBDV genome of rCu-1-p0, rCu-1-p12/B, and rCu-1-p12/B/7DMA characterized by RNA deep-sequencing.

IBDV segment	Genomic region	nt position	nt substitution <sup>a</sup>	aa substitution <sup>b</sup>	rCu-1-p0	rCu-1-p12/B			rCu-1-p12/B/7DMA		
						R1	R2	R3	R1	R2	R3
A	VP5	316*	<b>AUU:UUU</b>	Ile74Phe				11%			
		317*	<b>AUU:ACU</b>	Ile74Thr	8%						
		493*	<b>CGG:UGG</b>	Arg133Trp					12%		
		508*	<b>CGU:UGU</b>	Arg138Cys							38%
		<i>VP5 Mutation frequency (sub/10<sup>4</sup>nt)</i>				22.8	7.6			15.2	
	VP2	316*	<b>GGA:GGU</b>	Gly62Gly					11%		
		317*	<b>UUC:CUC</b>	Phe63Leu	8%						
		493*	<b>AAC:AAU</b>	Asn121Asn					12%		
		508*	<b>GCC:GCU</b>	Ala126Ala							38%
		795	<b>CCA:CUA</b>	Pro222Leu		58%				18%	
		1018	<b>AUU:AUC</b>	Ile296Ile							
		1282	<b>GUU:GUC</b>	Val384Val				8%			
		1369	<b>GUC:GUA</b>	Val413Val				7%			
	<i>VP2 Mutation frequency (sub/10<sup>4</sup>nt)</i>				6.5	8.7			6.5		
	VP4	2061	<b>CCC:CUC</b>	Pro644Leu							29%
		2169	<b>UGU:UAU</b>	Cys680Tyr		97%	62%	25%	44%	40%	14%
		2168	<b>UGU:CGU</b>	Cys680Arg				10%			
		2267	<b>GCC:ACC</b>	Ala713Thr			21%	35%		25%	
		2268	<b>GCC:GAC</b>	Ala713Asp						11%	
		2284	<b>GCA:GCG</b>	Ala718Ala				7%			
	<i>VP4 Mutation frequency (sub/10<sup>4</sup>nt)</i>				0	32			27.3		
	VP3	2531	<b>AUG:GUG</b>	Met801Val						19%	
		2736	<b>UUU:UCU</b>	Phe869Ser							10%
2785		<b>CCC:CCA</b>	Pro885Pro				9%				
2794		<b>CUA:CUG</b>	Leu888Leu				9%				
2824		<b>CCG:CCU</b>	Pro898Pro				8%				
2827		<b>GAC:GAU</b>	Asp899Asp				8%				
2896		<b>CUG:CUA</b>	Leu922Leu		37%	37%	36%	64%	28%	88%	
<i>VP3 Mutation frequency (sub/10<sup>4</sup>nt)</i>				0	26			21.6			
3'UTR	3205	<b>U:C</b>						95%	20%		
	3227	<b>C:A</b>			86%	20%	11%		13%		
	3227	<b>C:U</b>								21%	
	3229	<b>C:U</b>							13%		
	3230	<b>C:U</b>			8%		73%			78%	
	3230	<b>C:A</b>				38%			42%		
<i>Mean coverage</i>				69	56	62	41	14	53	26	
<i>Total number of SNVs</i>				1	24			21			
<i>Mean number of SNVs<sup>c</sup></i>				1	8			7.7			
<i>Mean number of Non-Synonymous-SNVs</i>				2	3			3.3			
<i>Mean number of Synonymous-SNVs</i>				0	3.7			2			
<i>Mutation frequency (sub/10<sup>4</sup> nt)<sup>d</sup></i>				3.1	24.5			21.5			
<i>Nucleotide diversity, π (× 10<sup>-4</sup>)</i>				0.5	7			7.2			
B	VP1	413	<b>AUU:ACU</b>	Ile101Thr						10%	
		516	<b>AUU:AUC</b>	Ile135Ile			8%				
		620	<b>AUG:ACG</b>	Met170Thr					15%		
		779	<b>GUG:GCG</b>	Val223Ala					13%		
		781	<b>CCA:UCA</b>	Pro224Ser				7%			
		1035	<b>AGU:AGC</b>	Ser308Ser					11%		
		1096	<b>ACA:GCA</b>	Thr329Ala					26%	100%	26%
		1255	<b>UUG:CUG</b>	Leu382Leu							7%
		2195	<b>AAG:AGG</b>	Lys695Arg	9%						

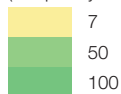
(Continued)

TABLE 2 | Continued

IBDV segment	Genomic region	nt position	nt substitution <sup>a</sup>	aa substitution <sup>b</sup>	rCu-1-p0	rCu-1-p12/B			rCu-1-p12/B/7DMA		
						R1	R2	R3	R1	R2	R3
		2355	<b>GUU</b> :GUC	Val748Val					12%		
		2363	<b>AAG</b> :AGG	Leu751Arg			8%				
		2370	<b>GAA</b> :GAG	Glu753Glu					8%		
		2511	<b>GCC</b> :GCU	Ala800Ala					100%		
		2682	<b>GCC</b> :GCU	Ala857Ala				8%			
		2705	<b>GUG</b> :GCG	Val865Ala							16%
		VP1 Mutation frequency (sub/10 <sup>4</sup> nt)			3.8	5			15.2		
		Mean coverage			34	60	79	56	23	76	39
		Total number of SNVs			1	4			12		
		Mean number of SNVs <sup>c</sup>			1	1.3			4		
		Mean number of Non-Synonymous-SNVs			1	0.7			2.3		
		Mean number of Synonymous-SNVs			0	0.7			1.7		
		Mutation frequency (sub/10 <sup>4</sup> nt) <sup>d</sup>			3.5	4.7			14.1		
		Nucleotide diversity, $\pi$ ( $\times 10^{-4}$ )			0.6	0.7			2.9		

Color legend

(Frequency in %)



<sup>a</sup>Nucleotide (nt) substitution column show in bold the nt replaced (on the left) by the new one (on the right) after passages in the corresponding untranslated (UTR) or coding regions. For coding regions, other nucleotides from the same codon are displayed.

<sup>b</sup>Amino acid (aa) substitution indicated in VP5 ORF, the polyprotein or VP1 ORF.

<sup>c</sup>Mean number of SNV (single nucleotide variant) was obtained by dividing the total number of SNVs by the number of replicates.

<sup>d</sup>To obtain mutation frequency per 10 000 nucleotides (nt) sequenced, mean number of SNVs was divided by the total genome length (3260 nt for segment A or 2827 nt for segment B) and then multiplied by 10 000 nt to display a more user-friendly number. Sub: substitutions.

R (replicate). Variant frequency is color-coded from yellow (frequency of 7%) to green (frequency of 100%). \*Mutations in the region belonging to both VP5 ORF and VP2 coding region.

and VP4. In contrast, a two-fold increase was apparent in rCu-1-p12/DF-1 VP2 CDR compared with to rCu-1-p12/DF-1/7DMA (Table 3).

In this segment, the mutation frequency and the nucleotide diversity (Table 3) were comparable for both viral stocks.

#### Analysis of segment B from rCu-1-p12/DF-1 and rCu-1-p12/DF-1/7DMA

In rCu-1-p12/DF-1, the observed mutation frequency for VP1 ORF was 1.3 sub/10<sup>4</sup> nt (Table 3), while in rCu-1-p12/DF-1/7DMA, this frequency increased 9 times (11.4 sub/10<sup>4</sup> nt). For segment B, in rCu-1-p12/DF-1/7DMA, the mutation frequency and the nucleotide diversity (Table 3) increased 9.8 and 11 times, respectively, in comparison with rCu-1-p12/DF-1.

#### Analysis of segments A and B from rCu-1-p5/ch

In segment A, mutation frequencies of 26 and 13.7 sub/10<sup>4</sup> nt were observed for VP2 and VP4, respectively. In segment B, the mutation frequency reached a value of 15.2 sub/10<sup>4</sup> nt. The mutation frequency as well as the nucleotide diversity (Table 3) were comparable between both segments.

The results in section 3.2. indicated that although serial passages were associated with the appearance of mutations in both segments, 7DMA seemed to specially target the viral polymerase VP1 as previously described in other viruses (Olsen et al., 2004; Zmurko et al., 2016), producing a higher increase in

the number of mutations and nucleotide diversity in segment B than in segment A.

## Dominant Mutations After Serial Passaging

In order to evaluate the relevance of chicken B cells as a cell system for IBDV replication and study the adaptability of virus to new conditions such as the presence of 7DMA, dominant mutations (that appeared at consensus levels, i.e., with frequencies higher than 50%) detected after passages in chickens and cells were further analyzed. To guide the reader, mutations in VP2, VP4 and VP3 CDRs are indicated as substitutions along the amino acid numbering of the polyprotein.

### rvv in Chicken B Cells

#### Dominant mutations in segment A from rvv-p12 and rvv-p12/7DMA

In rvv-p12, only one dominant mutation, observed in all replicates, was identified in VP2 CDR, inducing the Ala270Glu change (Table 1). In rvv-p12/7DMA, one dominant mutation was identified in all replicates in the same position 270, although that change encoded a threonine instead of a glutamic acid (Ala270Thr, Table 1). No mutation previously associated to cell culture adaptation, such as changes in VP2 positions 253, 279, 284 or 330, was detected in neither rvv-p12 nor rvv-p12/7DMA.

**TABLE 3 |** Analysis of variant frequencies and genetic variation in IBDV genome of rCu-1-p12/DF-1, rCu-1-p12/DF-1/7DMA, and rCu-1-p5/ch characterized by RNA deep-sequencing.

IBDV segment	Genomic region	nt position	nt substitution <sup>a</sup>	aa substitution <sup>b</sup>	rCu-1-p12/DF-1			rCu-1-p12/DF-1/7DMA			rCu-1-p5/ch
					R1	R2	R3	R1	R2	R3	
A	5'UTR	81	<b>U:C</b>							13%	
	VP5	283*	<b>CAC:UAC</b>	His63Tyr					11%		
		487*	<b>ACU:GCU</b>	Thr131Ala		11%					
	VP5 Mutation frequency (sub/10 <sup>4</sup> nt)				7.6			7.6			0
	VP2	283*	<b>GAC:GAU</b>	Asp51Asp					11%		
		487*	<b>GCA:GCG</b>	Ala119Ala		11%					
		610	<b>GUA:GUG</b>	Val160Val		21%					
		832	<b>AUU:AUC</b>	Ile234Ile				15%			
		876	<b>CAA:CGA</b>	Gln249Arg	25%						
		888	<b>CAC:CUC</b>	His253Leu							100%
		1063	<b>GAG:GAA</b>	Glu311Glu							8%
		1312	<b>GCC:GCU</b>	Ala394Ala		18%					
		1489	<b>AGG:AGA</b>	Arg453Arg							15%
		1555	<b>GAA:GAU</b>	Glu475Asp							40%
	VP2 Mutation frequency (sub/10 <sup>4</sup> nt)				8.7			4.3			26
	VP4	2169	<b>UGU:UAU</b>	Cys680Tyr			34%				15%
		2267	<b>GCC:ACC</b>	Ala713Thr							55%
	VP4 Mutation frequency (sub/10 <sup>4</sup> nt)				4.6			4.5			13.7
	VP3	2617	<b>CAA:CAG</b>	Gln829Gln			24%				
		2896	<b>CUG:CUA</b>	Leu922Leu	90%	59%	62%	83%	45%	42%	
VP3 Mutation frequency (sub/10 <sup>4</sup> nt)				17.3			13			0	
3'UTR	3229	<b>C:U</b>			31%			18%			
	3230	<b>C:U</b>					11%				
	3230	<b>C:G</b>						17%			
Mean coverage				349	422	234	93	66	119	71	
Total number of SNVs				11			9			5	
Mean number of SNVs <sup>c</sup>				3.7			3			5	
Mean number of Non-Synonymous-SNVs				1			0.7			3	
Mean number of Synonymous-SNVs				2.3			1.7			2	
Mutation frequency (sub/10 <sup>4</sup> nt) <sup>d</sup>				11.2			9.2			15.3	
Nucleotide diversity, π (×10 <sup>-4</sup> )				3.9			2.9			4.3	
B	5'UTR	109	<b>A:G</b>						10%		
	VP1	818	<b>ACG:AUG</b>	Thr236Met							8%
		1096	<b>ACA:GCA</b>	Thr329Ala				87%	96%	100%	
		1153	<b>AUC:GUC</b>	Ile348Val							8%
		1371	<b>GGU:GGC</b>	Gly420Gly				10%			
		1461	<b>AAU:AAC</b>	Asn450Asn				7%			
		1578	<b>ACG:ACA</b>	Thr489Thr						8%	
		2346	<b>CAA:CAG</b>	Gln745Gln							14%
		2481	<b>GCC:GCU</b>	Ala790Ala							18%
		2511	<b>GCC:GCU</b>	Ala800Ala		9%			31%	84%	
		2705	<b>GUG:GCG</b>	Val865Ala				12%			
	VP1 Mutation frequency (sub/10 <sup>4</sup> nt)				1.3			11.4			15.2
	Mean coverage				1822	1336	909	196	134	210	83
Total number of SNVs				1			10			4	
Mean number of SNVs <sup>c</sup>				0.3			3.3			4	
Mean number of Non-Synonymous-SNVs				0			1			2	
Mean number of Synonymous-SNVs				0.3			1.7			2	

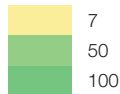
(Continued)

TABLE 3 | Continued

IBDV segment	Genomic region	nt position	nt substitution <sup>a</sup>	aa substitution <sup>b</sup>	rCu-1-p12/DF-1			rCu-1-p12/DF-1/7DMA			rCu-1-p5/ch
					R1	R2	R3	R1	R2	R3	
		Mutation frequency ( $sub/10^4 nt$ ) <sup>d</sup>				1.2			11.8		14.1
		Nucleotide diversity, $\pi$ ( $\times 10^{-4}$ )				0.2			2.2		2.9

Color legend

(Frequency in %)



<sup>a</sup>Nucleotide (nt) substitution column show in bold the nt replaced (on the left) by the new one (on the right) after passages in the corresponding untranslated (UTR) or coding regions.

<sup>b</sup>Amino acid (aa) substitution indicated in VP5 ORF, the polyprotein or VP1 ORF.

<sup>c</sup>Mean number of SNV (single nucleotide variant) was obtained by dividing the total number of SNVs by the number of replicates.

<sup>d</sup>To obtain mutation frequency per 10 000 nucleotides (nt) sequenced, mean number of SNVs was divided by the total genome length (3260 nt for segment A or 2827 nt for segment B) and then multiplied by 10 000 nt to display a more user-friendly number. Sub: substitutions.

R (replicate). Variant frequency is color-coded from yellow (frequency of 7%) to green (frequency of 100%). \*Mutations in the region belonging to both VP5 ORF and VP2 coding region.

### Dominant mutations in segment B from rrv-p12 and rrv-p12/7DMA

In rrv-p12, one dominant mutation located in the nucleotide position 2764 (**Table 1**) was detected in the 3'UTR. Since the UTRs play an important role during the replication and translation of IBDV (Boot and Pritz-Verschuren, 2004), their secondary structures were analyzed. The mutation in nucleotide position 2764 showed a branch stem-loop structure as well as in rrv-p0 (**Figures 2A,B**). Although RNA structure prediction revealed a conformational change, where the mutation C2764U provoked an extension in the stem located in the stem-loop into 2767–2777 region (**Figure 2B**), both structures conserved the stem-loop located into the 2801–2827 region previously described (Boot and Pritz-Verschuren, 2004).

In rrv-p12/7DMA, a single dominant mutation in VP1 ORF was observed in all replicates, inducing the Thr329Ala change (**Table 1**).

### rCu-1 in Cells and Chickens

#### Dominant mutations in segment A from rCu-1-p12/B and rCu-1-p12/B/7DMA

In rCu-1-p12/B, no SNVs was dominant in all three replicates, however, dominant SNVs were observed in certain replicates (**Table 2**). A dominant mutation in VP2 CDR and another in VP4 CDR were observed, resulting in the Pro222Leu and Cys680Tyr mutations, respectively (**Table 2**). Two dominant SNVs were located in 3'UTR, resulting in the C3227A and C3230U mutations (**Table 2**), although they did not produce a conformational change in the 3'UTR structure, which showed a branch stem-loop structure as well as in rCu-1-p0 (**Figures 2C,D**). In this prediction, the two-nucleotide substitutions, C3227A and C3230U, present in rCu-1-p12/B genome, were supposed to coexist in the same RNA molecule due to their, similarly, high frequency in two given replicates (R1 and R3, **Table 2**).

In rCu-1-p12/B/7DMA, the dominant, synonymous mutation Leu922Leu was detected in VP3 CDR (**Table 2**). Two dominant SNVs were located in 3'UTR, resulting in the U3205C and

C3230U mutations: since none of those mutations coexisted in any given replicate, each mutation was considered in a distinct RNA molecule for RNA secondary structure determination. The mutation U3205C provoked the apparition of an extra stem-loop into the 3170–3183 region (**Figure 2E**), while C3230U did not modify the RNA structure with respect to the structure shown by rCu-1-p0 (**Figure 2C**). All these structures (**Figures 2C–F**) have in common that they conserve the stem-loop located into the 3239–3260 region, as previously described (Boot and Pritz-Verschuren, 2004). For each prediction, two additional structural variations were computed as possible: all the predicted structures displayed the same branch stem-loop structure, therefore only the most thermodynamically stable structures are presented.

#### Dominant mutations in segment B from rCu-1-p12/B and rCu-1-p12/B/7DMA

No dominant mutation was detected in rCu-1-p12/B. However, the 7DMA treatment induced the Thr329Ala and Ala800Ala mutations in VP1 ORF. Although Thr329Ala emerged as a dominant change, with a frequency of 100%, it was only observed in one replicate (**Table 2**).

#### Dominant mutations in segment A from rCu-1-p12/DF-1 and rCu-1-p12/DF-1/7DMA

Only the Leu922Leu synonymous mutation in VP3 CDR reached consensus levels in rCu-1-p12/DF-1 and rCu-1-p12/DF-1/7DMA (**Table 3**).

#### Dominant mutations in segment B from rCu-1-p12/DF-1 and rCu-1-p12/DF-1/7DMA

No dominant mutation was detected in rCu-1-p12/DF-1. In rCu-1-p12/DF-1/7DMA, the Thr329Ala change was observed in all replicates, while Ala800Ala change was present in one replicate (**Table 3**).

#### Dominant mutations in segment A and B from rCu-1-p5/ch

In segment A, two dominant mutations were detected, one in hVP2 (His253Leu), with 100% of variant frequency and the second one in VP4 CDR (Ala713Thr), with 55% variant frequency (**Table 3**). The latter was also detected in two

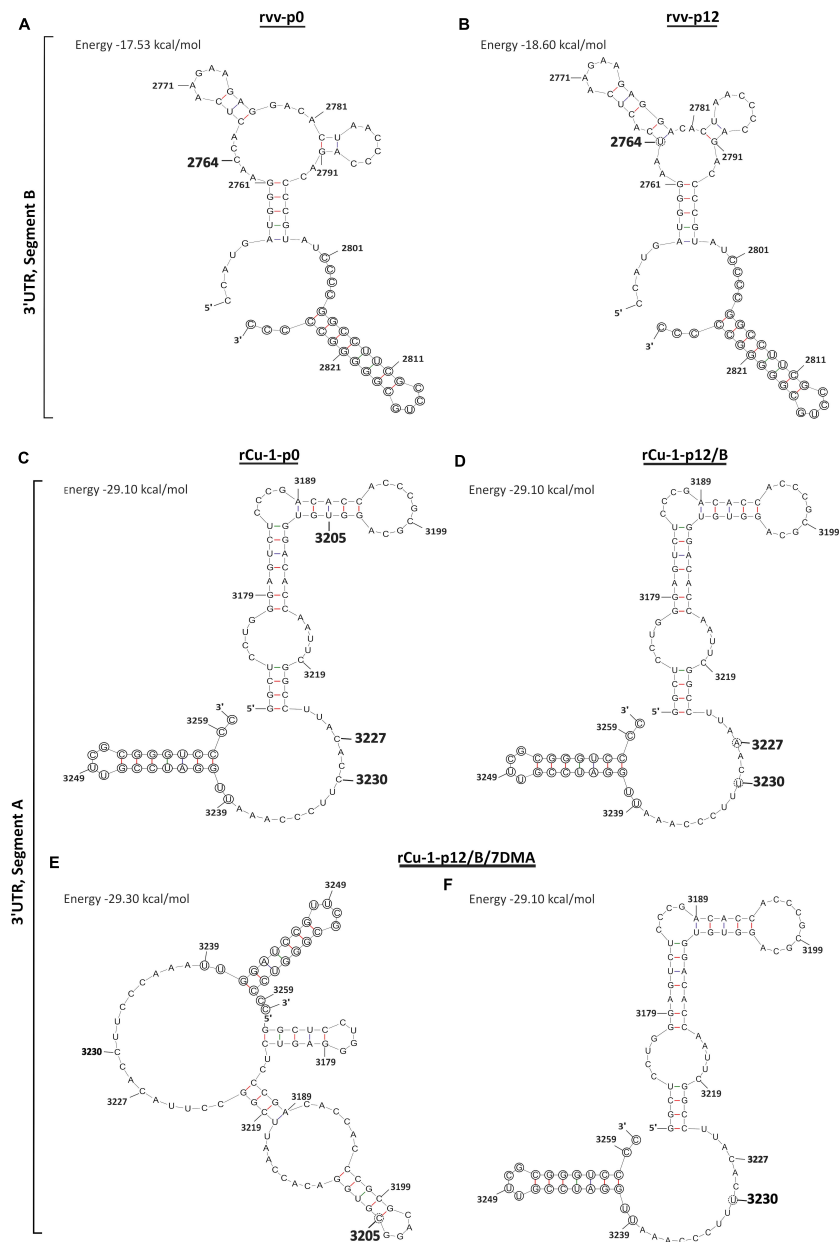


**FIGURE 2 |** Predictions of RNA secondary structures in the 3'UTR in IBDV genome. **(A)** The original 3'UTR sequence of segment B in *rvv-p0* featuring in bigger bold number the mutated nucleotide position after passaging. **(B)** The 3'UTR sequence of segment B in *rvv-p12*, featuring in a dotted circle the nucleotide substitution. **(C)** The original 3'UTR sequence of segment A in *rCu-1-p0* featuring in bigger bold numbers the mutated nucleotide positions after passaging. **(D)** The 3'UTR sequence of segment A in *rCu-1-p12/B*, featuring in a dotted circle the nucleotide substitution. **(E,F)** The 3'UTR sequence of segment A in *rCu-1-p12/B/7DMA*, featuring in dotted circles the nucleotide substitutions. In circles, conserved regions in 3'UTR sequences. Energy levels for each structure are given in kcal/mol in brackets.

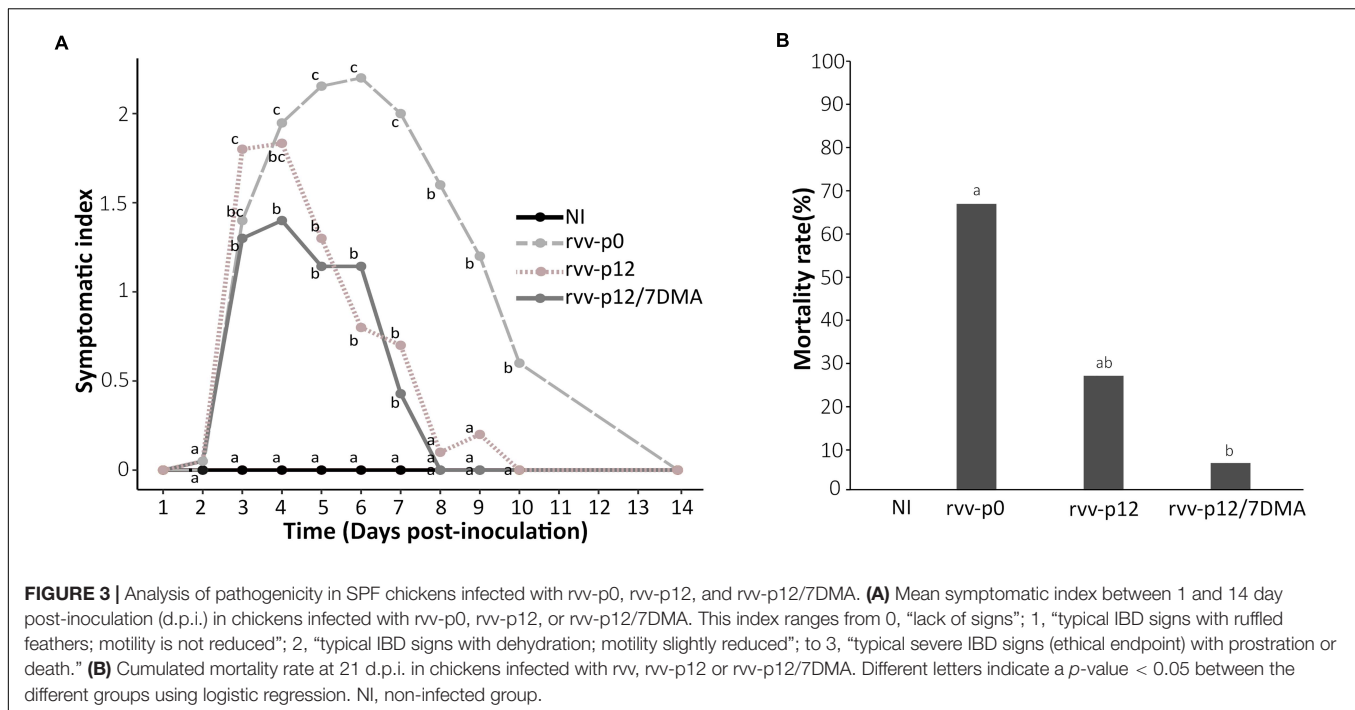
replicates in *rCu-1-p12/B* but at frequencies lower than 50% (21 and 35%, respectively, **Table 3**). No dominant mutation was detected in segment B.

The results in section 3.3 showed that few dominant mutations were detected after passages in non-coding regions together with non-synonymous mutations in VP2 (positions 222, 253 and 270) and in VP4 (positions 680 and 713) CDRs. In addition, the mutation Thr329Ala in VP1 ORF

specifically appeared after 7DMA treatment in both cell types and IBDV strains.

### Pathogenicity of *rvv-p0*, *rvv-p12*, and *rvv-p12/7DMA* in SPF Chickens

In order to get further insight into the impact of the mutant spectra obtained after passaging on virulence, the pathogenicity



of the stocks of rvv-p12 or rvv-p12/7DMA was assessed in SPF chickens and compared with rvv-p0, which is a genetically homogenous inoculum. For this purpose, among three replicates for each condition, the replicate with a representative number of variants and dominant mutations was selected (Table 1). Accordingly, replicates R1 for both rvv-p12 (with median percentages for the dominant mutations Ala270Glu in VP2 and C2764U in 3'UTR in segment B) and rvv-p12/7DMA (with the highest variant frequency for the mutation Thr329Ala in VP1, 99%) were chosen to carry out the animal trial in SPF chickens using the standard protocol previously described (Le Nouen et al., 2012). Neither clinical signs nor mortality were observed in non-infected control chickens (NI, Figure 3A). In contrast, inoculation with rvv-p0 and rvv-p12 resulted in mild to severe clinical signs, characterized by diarrhea, prostration and ruffled feathers, with a mean symptomatic index of 1.95 and 1.83 at 4 d.p.i., inducing 67 and 27% of mortality, respectively (Figure 3B). In contrast, rvv-p12/7DMA resulted in 7% of mortality associated with mild clinical signs and a mean symptomatic index of 1.4 at 4 d.p.i. The statistical analysis showed that although the mortality induced by rvv-p0 was higher than that induced by rvv-p12, it did not differ significantly. In contrast, the mortality rate produced by rvv-p0 differed significantly from the mortality induced by rvv-p12/7DMA, indicative of attenuation of the later *in vivo*.

To study bursal atrophy, gross changes in spleen and chicken B cell depletion, analysis of bursal-to-body weight [b/B] ratio, spleen-to-body-weight ratio [s/B] and counting of blood cells were carried out, respectively. b/B ratio did not reveal any significant differences at 4 d.p.i (Figure 4A) between the four different groups. However, b/B ratio showed marked bursal atrophy at 21 d.p.i in all three challenged groups, with an average 4.4 fold reduction in comparison with mock-infected birds (Figure 4B). In contrast, an increase was globally observed

for s/B in infected groups (Figures 4C,D): this increase was not statistically significant for the rvv-p0 group (median value: 1.57 % versus 1.36 % for NI), unlike the rvv-p12 and rvv-p12/7DMA groups; for the latter, marked splenomegaly was observed with a median value of 2.77%. Splenomegaly was no longer visible at 21 d.p.i. except for the rvv-p0 group (Figure 4D).

To count the number of circulating chicken B cells, blood samples were taken from chickens in each group. In general, chicken B cells depletion was observed in all the infected groups (Figures 4E,F). At 2 d.p.i., a reduced chicken B cell concentration was found in birds from the rvv-p0 group (median cell count of 155.5/ $\mu$ L) in comparison with birds from NI (median cell count of 2279/ $\mu$ L). This concentration appeared significantly higher than that of birds from rvv-p12 (median cell count below the detection limit of 5/ $\mu$ L) and rvv-p12/7DMA (median cell count of 6.5/ $\mu$ L) groups (Figure 4E). At 21 d.p.i., a comparable recovery in the number of chicken B cells was observed in the three infected groups, although all of them appeared 10-fold below the concentration of B cells detected in the NI group (Figure 4F). A similar pattern of early reduction compared with NI birds was observed for other blood cell types, with mild cell-type specific variations (Supplementary Figure 2). Namely, for T cells and thrombocytes, a significant reduction was apparent in all groups at 2 d.p.i. At the same time, a reduction in the number of monocytes was only significant for rvv-p12 and rvv-p12/7DMA groups. At 21 d.p.i., cells numbers from infected groups tended to go back to values closer to that of control birds.

To determine the viral load in BF and to monitor cloacal viral shedding, viruses from bursae were biologically titrated and viral RNA from cloacal swabs were quantified. High and similar bursal viral titers were detected among the three challenged groups at 4 d.p.i. (Figure 4G). In general, the cloacal viral

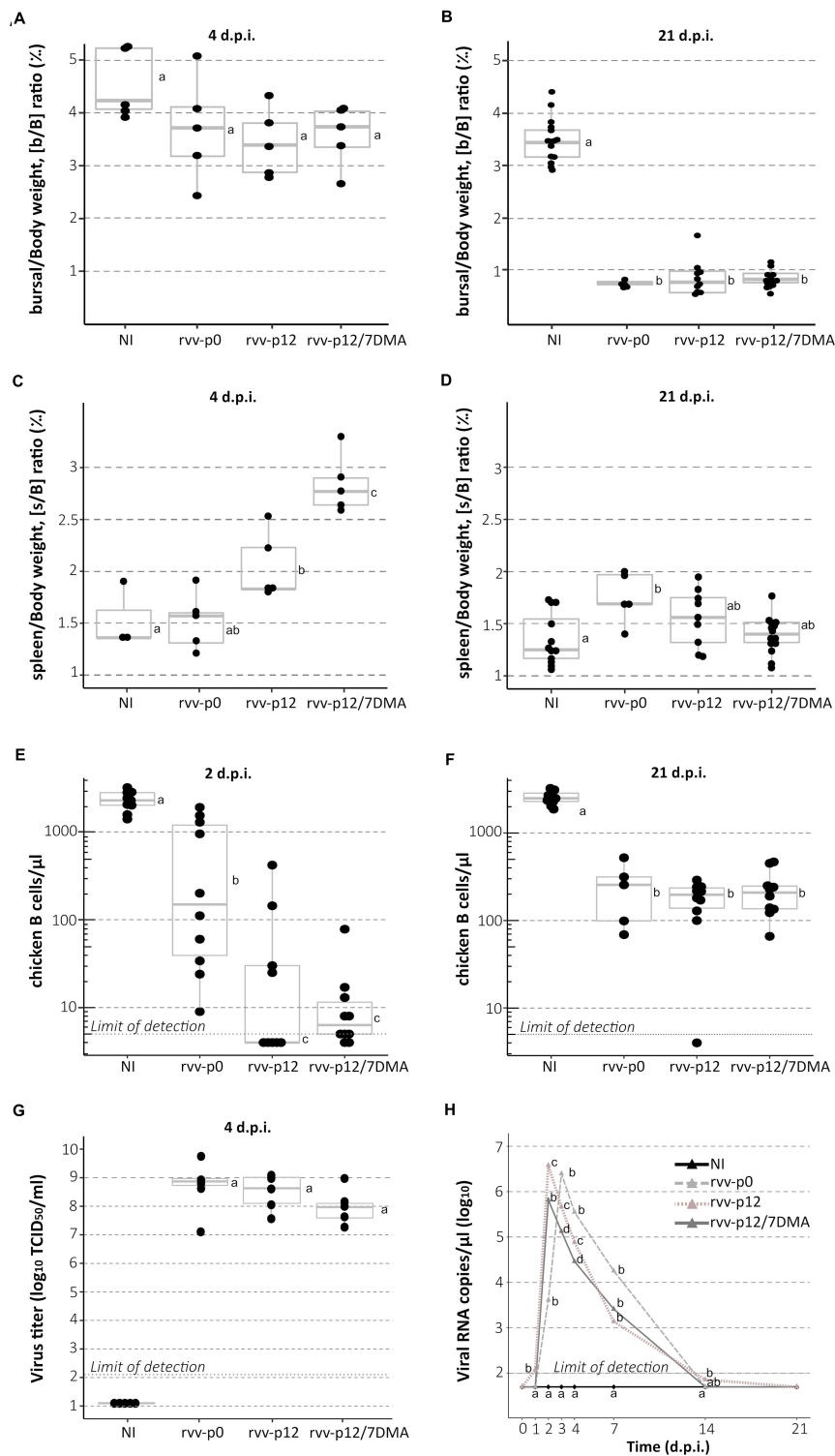


**FIGURE 4** | Bursal-to-body weight ratio, spleen-to-body-weight ratio, chicken B cells counting, viral load in Bursa of Fabricius and viral shedding in chickens infected with rvv-p0, rvv-p12, or rvv-p12/7DMA. **(A,B)** Bursal-to-body weight [b/B] ratio (%) at 4 ( $n = 5$  chickens per group) and 21 days (at least 5 chickens per group) post-inoculation (d.p.i.). **(C,D)** Spleen-to-body-weight [s/B] ratio (%) at 4 ( $n = 5$  chickens per group) and 21 d.p.i. (at least 5 chickens per group). **(E,F)** Chicken B cell concentration in blood at 2 and 21 d.p.i. ( $n = 10$  chickens per group except for the rvv-p0 group). **(G)** Virus titer at day 4 in Bursa of Fabricius [ $\log_{10}$  TCID<sub>50</sub>/mL),  $n = 5$  chickens per group). For **A–G**, points represent individual values; boxplots indicate median and interquartile range. **(H)** Median viral shedding per group (in viral RNA copies/ $\mu$ L) at day 0–4, 7, 14, and 21 from cloacal swabs. For all graphs, different letters indicate a  $p$ -value  $< 0.05$  between the different groups using Kruskal-Wallis test followed by Fisher's least significant difference test with Holm adjustment method for multiple comparisons. NI, non-infected group.

excretion of rvv-p12/7DMA, measured by qRT-PCR, remained lower than those found in the other two rvv groups, reaching a reduction of 1 log<sub>10</sub> (copies/μL RNA) at 3 and 4 d.p.i compared to the rvv-p0 group (**Figure 4H**). rvv-p12 viral shedding was similar to that detected in the rvv-p0 group. Although the three challenge viruses seem to display similar replication in the BF, these results collectively indicate that rvv-p12/7DMA, unlike rvv-p12, shows a reduced pathogenicity in comparison with the parental rvv strain.

### Variant Frequency, Dominant Mutations, Mutation Frequency and Nucleotide Diversity ( $\pi$ ) in rvv-p0/BF, rvv-p12/BF, and rvv-p12/7DMA/BF

In order to characterize the viral population during infection after inoculation with rvv-p0, rvv-p12 and rvv-p12/7DMA, viral RNA were extracted from the BF sampled at 4 d.p.i. of chicken inoculated with these viruses. These viral RNA were reverse transcribed, both genomic segments A and B were PCR-amplified and subsequently subjected to DNaseq together with the inoculum of each group. Complete PCR amplification of IBDV genome did not work, neither with viral inocula nor with some samples from BF (**Table 4** shows for which samples complete genome RT-PCR was successful and which ones were used to analysis). For those samples, partial genome RT-PCR was attempted instead, producing amplicons that spanned the regions where dominant mutations were detected by RNA deep-sequencing. With this second-choice strategy, amplification was successful for the three inocula and failed again for the bursa-derived samples.

Similar number of SNVs and variant frequencies were detected between rvv-p0, rvv-p12 and rvv-p12/7DMA inocula sequenced by RNA deep-sequencing and DNaseq (**Table 1** and **Supplementary Table 2**, respectively). To avoid bias, mutation frequency and nucleotide diversity parameters presented in **Table 4** were normalized to the number of samples and the length of region sequenced.

#### Analysis of Segment A From rvv-p0/BF, rvv-p12/BF, and rvv-p12/7DMA/BF

No mutation was found in rvv-p0 inoculum (**Supplementary Table 4**) while eight new SNVs were detected in VP2 CDR in rvv-p0/BF, distributing in two nucleotide positions (**Table 4**). VP2 CDR reached a mutation frequency of 13 sub/10<sup>4</sup> nt.

New SNVs were detected in rvv-p12/BF with respect to rvv-p12 (**Table 4**), distributing in eight nucleotide positions in VP2 CDR, three in VP4 CDR, six in VP3 CDR and one in the 3'UTR. VP2, VP4 and VP3 reached mutation frequencies of 35.8, 27.3, and 16.2 sub/10<sup>4</sup> nt, respectively.

New SNVs emerged in rvv-p12/7DMA/BF with respect to rvv-p12/7DMA (**Table 4**), distributing in three nucleotide positions in the 5'UTR, one in VP5 ORF, one in in the region belonging to both VP5 ORF and VP2 CDR, nine in VP2 CDR and two in VP3 CDR. VP5, VP2, VP4 and VP3

reached mutation frequencies of 8.9, 35.2, 5.5, and 5.2 sub/10<sup>4</sup> nt, respectively.

Concerning dominant mutations, only two, Ala270Glu or Ala270Thr, were detected in VP2 CDR in rvv-p12/BF or rvv-p12/7DMA/BF, respectively, in most of chickens at frequencies similar to their corresponding inocula (**Table 4** and **Supplementary Table 2**). Interestingly, two chickens out of five from the rvv-p12/7DMA/BF group presented both Ala270Glu and Ala270Thr mutations (**Table 4**). No dominant mutation was detected in rvv-p0/BF.

In this segment, the values for the mean number of SNVs, the mean numbers of NS- and S-SNVs, the mutation frequency as well as the nucleotide diversity (**Table 4**) were always higher for rvv-p12/BF and rvv-p12/7DMA/BF than for rvv-p0/BF. These parameters were similar between rvv-p12/BF and rvv-p12/7DMA/BF, with the exception for the mean number of NS-SNVs, which was 2 times higher in rvv-p12/BF than in rvv-p12/7DMA/BF.

#### Analysis of Segment B From rvv-p0/BF, rvv-p12/BF, and rvv-p12/7DMA/BF

No mutation was found in rvv-p0 (**Supplementary Table 4**), while three new SNVs were detected in rvv-p0/BF. Two mutations were located in the 5'UTR (in one nucleotide position) and one in VP1 ORF (**Table 4**). The latter reached a mutation frequency of 2.5 sub/10<sup>4</sup> nt.

New SNVs were detected in rvv-p12/BF with respect to rvv-p12, distributing in two nucleotide positions in the 5'UTR and three in VP1 ORF (**Table 4**). VP1 ORF mutation frequency was similar to that found in rvv-p0/BF.

The new SNVs found in rvv-p12/7DMA/BF with respect to rvv-p12/7DMA were distributed in one nucleotide position in the 5'UTR and three in VP1 ORF (**Table 4**). The mutation frequency in VP1 ORF increased 4.5 and 3 times with respect to those detected in rvv-p0/BF and rvv-p12/BF, respectively.

Concerning dominant mutations, one dominant mutation (Phe138Phe) was found in rvv-p0/BF, although only in one chicken: this variant produced a synonymous mutation (**Table 4**). One dominant mutation was detected in rvv-p12/BF in the 3'UTR, but its frequency could not be quantified in rvv-p12 inoculum after DNaseq, due to the partial amplification strategy used for this inoculum. However, this mutation was detected in the three replicates when rvv was passaged 12 passages in chicken B cells (**Table 1**), excluding its appearance after the infection of chickens. Four out four chickens in the rvv-p12/7DMA/BF presented the Thr329Ala mutation in VP1 ORF with variant frequencies similar to those found in the rvv-p12/7DMA inoculum (**Table 4** and **Supplementary Table 2**).

Although infection in chickens was carried out in the absence of 7DMA, rvv-p12/7DMA/BF showed the highest nucleotide diversity and mutation frequency in segment B without reversion in VP1 at position 329 (**Table 4**). The latter suggests that this mutation shows a relative stability and may contribute to the reduced pathogenicity observed in chickens infected with rvv-p12/7DMA.

**TABLE 4** | Analysis of variant frequencies and genetic variation in IBDV genome of rvv-p0, rvv-p12, and rvv-p12/7DMA recovered from Bursa of Fabricius.

IBDV segment	Genomic region	nt position	nt substitution <sup>a</sup>	aa substitution <sup>b</sup>	rvv-p0/BF					rvv-p12/BF					rvv-p12/7DMA/BF					
					ch1	ch2	ch3	ch4	ch5	ch1	ch2	ch3	ch4	ch5	ch1	ch2	ch3	ch4	ch5	
A	5'UTR	24 <sup>†</sup>	<b>G:A</b>																9%	
		35 <sup>†</sup>	<b>G:A</b>											7%						
		50	<b>A:G</b>																17%	
		53	<b>C:U</b>												8%	10%				
		54	<b>C:U</b>														16%			
	75 <sup>†</sup>	<b>U:C</b>													10%					
	VP5	126 <sup>†</sup>	<b>CGC:CGU</b>	Arg14Arg															15%	
		424 <sup>†</sup>	<b>CUG:UUG</b>	Leu114Leu															8%	
	<i>VP5 Mutation frequency (sub/10<sup>4</sup>nt)</i>					0					0					8.9				
	VP2	424 <sup>†</sup>	<b>UAC:UAU</b>	Tyr98Tyr																8%
		751 <sup>†</sup>	<b>ACC:ACU</b>	Thr207Thr																9%
		786 <sup>†</sup>	<b>CAG:CUG</b>	Gln219Leu																
		795	<b>GCA:GUA</b>	Ala222Val																
		835 <sup>†</sup>	<b>GAU:GAC</b>	Asp235Asp																12%
		869 <sup>†</sup>	<b>GUG:AUG</b>	Val247Met																7%
938		<b>GCG:ACG</b>	Ala270Thr																	
939		<b>GCG:GAG</b>	Ala270Glu																	
1189 <sup>†</sup>		<b>GCU:GCC</b>	Ala353Ala																	8%
1510 <sup>†</sup>		<b>UCU:UCG</b>	Ser460Ser																	
1511 <sup>†</sup>		<b>ACA:GCA</b>	Thr461Ala																	
1528 <sup>†</sup>		<b>GCC:GCG</b>	Ala466Ala																	
1530 <sup>†</sup>		<b>GCU:GGU</b>	Ala467Gly																	
1537 <sup>†</sup>	<b>CUA:CUG</b>	Leu469Leu																		
1561 <sup>†</sup>	<b>GUA:GUG</b>	Val477Val																		
1566 <sup>†</sup>	<b>UAC:UGC</b>	Tyr479Cys																		
1649 <sup>†</sup>	<b>AGG:GGG</b>	Arh507Gly																		
<i>VP2 Mutation frequency (sub/10<sup>4</sup>nt)</i>					13					35.8					35.2					
VP4	2023 <sup>†</sup>	<b>GAU:GAA</b>	Asp631Glu																	
	2336 <sup>†</sup>	<b>UAC:CAC</b>	Tyr736His																	
	2351	<b>UAC:CAC</b>	Tyr741His																	
	2378 <sup>†</sup>	<b>UAC:CAC</b>	Tyr750His																	
<i>VP4 Mutation frequency (sub/10<sup>4</sup>nt)</i>					0					27.3					5.5					
VP3	2419 <sup>†</sup>	<b>CCC:CCU</b>	Pro763Pro																	
	2642 <sup>†</sup>	<b>UAC:CAC</b>	Tyr838His																	
	2643 <sup>†</sup>	<b>UAC:UGC</b>	Try838His																	
	2840 <sup>†</sup>	<b>UAC:CAC</b>	Tyr904His																	
	2895 <sup>†</sup>	<b>CUA:CCA</b>	Leu922Pro																	
	2935 <sup>†</sup>	<b>GCA:GCG</b>	Ala935Ala																	
	2947 <sup>†</sup>	<b>CAA:CAG</b>	Gln939Gln																	
3151 <sup>†</sup>	<b>UCU:UCC</b>	Ser1007Ser																		
<i>VP3 Mutation frequency (sub/10<sup>4</sup>nt)</i>					0					16.2					5.2					

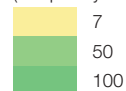
(Continued)

TABLE 4 | Continued

IBDV segment	Genomic region	nt position	nt substitution <sup>a</sup>	aa substitution <sup>b</sup>	rvv-p0/BF					rvv-p12/BF					rvv-p12/7DMA/BF					
					ch1	ch2	ch3	ch4	ch5	ch1	ch2	ch3	ch4	ch5	ch1	ch2	ch3	ch4	ch5	
	3'UTR	3223 <sup>†</sup>	<b>C:U</b>									32%								
	Mean coverage					161411	NA	390132	2976923	385669	NA	305072	321401	125022	331745	152334	2884305	378067	218127	359947
	Total number of SNVs															39				
	Mean number of SNVs <sup>c</sup>															8				
	Mean number of Non-Synonymous-SNVs															3.4				
	Mean number of Synonymous-SNVs															3.2				
	Mutation frequency (sub/10 <sup>4</sup> nt) <sup>d</sup>															24.5				
Nucleotide diversity, $\pi$ ( $\times 10^{-4}$ )															5.3					
B	5'UTR	10 <sup>†</sup> 66 <sup>†</sup>	<b>G:C</b> <b>G:U</b>			13%	9%			15%				18%	22%			10%	24%	
	VP1	525 <sup>†</sup>	UUU:UUC	Phe138Phe			81%													
		1096	ACA:GCA	Thr329Ala											98%		98%	99%	99%	
		1440 <sup>†</sup>	GAU:GAC	Asp443Asp											20%			7%		
		1638 <sup>†</sup>	CAA:CAG	Gln509Gln							7%							31%		
		1641 <sup>†</sup>	CCU:CCC	Pro510Pro																
		2136 <sup>†</sup>	GCU:GCC	Ala675Ala											21%					
		2280	GGU:GGC	Gly723Gly											11%		8%	12%	50%	
		2499 <sup>†</sup>	GAA:GAG	Glu796Glu							7%									
	2571 <sup>†</sup>	CCA:CCG	Pro820Pro										8%							
VP1 Mutation frequency (sub/10 <sup>4</sup> nt)					2.5					3.8					11.4					
3'UTR	2764	<b>C:U</b>								98%		94%	64%	12%		32%	9%			
Mean coverage					143425	NA	110280	141348	NA	NA	183709	NA	177150	160257	122381	NA	115343	93352	139004	
Total number of SNVs					3					8					18					
Mean number of SNVs <sup>c</sup>					1					2.7					4.5					
Mean number of Non-Synonymous-SNVs					0					0					1					
Mean number of Synonymous-SNVs					0.3					0.7					2					
Mutation frequency (sub/10 <sup>4</sup> nt) <sup>d</sup>					3.6					9.4					15.9					
Nucleotide diversity, $\pi$ ( $\times 10^{-4}$ )					0.8					1.9					3.6					

Color legend

(Frequency in %)



The Bursae of Fabricius (BF) from 5 SPF chickens (ch) infected with rvv-p0, rvv-p12, or rvv-p12/7DMA were harvested at 4 days post-inoculation (d.p.i.) and processed to obtain viral stocks: rvv-p0/BF, rvv-p12/BF, and rvv-p12/7DMA/BF. These viral stocks were subjected to DNAseq.

<sup>a</sup>Nucleotide (nt) substitution column show in bold the nt replaced (on the left) by the new one (on the right) after passages in the corresponding untranslated (UTR) or coding regions. For coding regions, other nucleotides from the same codon are displayed.

<sup>b</sup>Amino acid (aa) substitution indicated in VP5 ORF, the polyprotein or VP1 ORF.

<sup>c</sup>Mean number of SNV (single nucleotide variant) was obtained by dividing the total number of SNVs or mutations by the number of the replicates.

<sup>d</sup>To obtain mutation frequency per 10 000 nt sequenced, mean number of SNVs was divided by the total length sequenced genome (3260 nt for segment A or 2827 nt for segment B) and then multiplied by 10 000 to display a number more user-friendly. Sub, substitutions.

Variant frequency is color-coded from yellow (frequency of 7%) to green (frequency of 100%). \*Mutations in the region belonging to both VP5 ORF and VP2 coding region. <sup>†</sup>New SNVs detected after DNAseq.

Some samples were not amplified (NA) or nor analyzed (NAn), see in the text for detailed information.

**TABLE 5** | Occurrence of mutations observed following experimental passages in naturally occurring IBDV genomes.

IBDV segment	Viral protein	aa substitution <sup>a</sup>	Virus stock	number of samples where the substitution was found/total	Other IBDV strains with similar residues <sup>b</sup>	
A	VP5	Ser7Gly	rvv-p12	1/3	Faragher 52/70 (cv, HG974565.1); USC2003 (vv, KU183665.1); USC2010 (vv, KU183667.1)	
	VP5	His63Tyr	rCu-1-p12/DF-1/7DMA	1/3	23/82 (serotype II, Z21971.1)	
	VP5	Ile74Phe	rCu-1-p12/B	1/3	Phenylalanine conserved in vvIBDV strains	
	VP5	Thr131Ala	rCu-1-p12/DF-1	1/3	GX-NNZ-11 (vv, JX134483.1)	
	VP5	Arg133Trp	rCu-1-p12/B/7DMA	1/3	Tryptophane conserved in vvIBDV strains	
	VP2	*Pro222Leu	rCu-1-p12/B	1/3	160019 (reassortant isolate, KY610529.1)	
	VP2	Gln249Arg	rCu-1-p12/DF-1	1/3	IC-IBDV-Br (KC603937.1); P2 (cv, X84034.1); Gt (cv, DQ403248.1)	
	VP2	*Ala270Glu	rvv-p12	3/3	UPM94/273 (vv, AF527039.1); OH (serotype II, U30818.1)	
	VP2	*Ala270Thr	rvv-p12/7DMA	3/3	Threonine highly conserved in vvIBDV strains	
	VP4	*Cys680Tyr	rCu-1-p12/B, rCu-1-p12/B/7DMA, rCu-1-p12/DF-1, rCu-1-p12/DF-1/7DMA	8/12	Tyrosine highly conserved in vvIBDV strains	
	VP4	Cys680Arg	rCu-1-p12/B	1/3	23/82 (serotype II, Z21971.1)	
	VP4	*Ala713Thr	rCu-1-p5/ch, rCu-1-p12/B, rCu-1-p12/B/7DMA	4/7	Threonine presents in all sequences analyzed	
	VP4	Tyr741His	rvv-p12, rvv-p12/7DMA	4/6	100056 (reassortant isolate, KU234528.1)	
	B	VP1	*Thr329Ala	rvv-p12/7DMA, rCu-1-p12/B/7DMA, rCu-1-p12/DF-1/7DMA	9/9	IBD13HeB01 (reassortant isolate, AKD94180.1)
		VP1	Val865Ala	rCu-1-p12/B/7DMA, rCu-1-p12/DF-1/7DMA	2/6	HBDY-1 (KX592159.1); OH (serotype II, U30819.1)

<sup>a</sup>Amino acid (aa) substitution indicated using numbering of VP5 ORF, polyprotein or VP1 ORF.

<sup>b</sup>The IBDV classification belonging to serotype I [classical virulent (cv); very virulent (vv)], serotype II or defined as a reassortant isolate was indicated when it was possible. In brackets, Genbank accession numbers.

\*Dominant mutations.

## Analysis of Naturally Occurring IBDV Genomes for the Occurrence of Mutations Obtained After Passaging

To investigate if the mutations found in the present study after passages in chicken B cells, DF-1 cells and chickens could be present in other IBDV strains, full length sequences of segments A and B of IBDV were downloaded from Genbank database. A maximum of 192, 123 and 152 sequences were analyzed, corresponding to VP5, polyprotein and VP1 sequences, respectively (Table 5).

### In Segment A, Regardless of 7DMA Treatment

In rvv, 4 different NS-SNVs detected at p12 were present in other IBDV strains, belonging to classical virulent, very virulent strains, reassortant isolates and strains of serotype II (Table 5). Among these four, only 2 were dominant: Ala270Glu and Ala270Thr.

In rCu-1, 6 and 4 several NS-SNVs detected at p12 in chicken B cells and DF-1 cells, respectively, and one NS-SNV detected

at p5 in chickens were present and observed in various strains as well as in rvv. Two mutations detected in VP5 (Ile74Phe and Arg133Trp) as well as the dominant mutation in VP4 (Cys680Tyr) appeared very conserved in very virulent strains. The acquisition of those residues, present in vvIBDV strains, could thus be beneficial during rCu-1 passages.

### In Segment B

Only 2 different SN-SNVs detected under 7DMA treatment in rvv and rCu-1 were present in naturally occurring IBDV genomes. The acquisition of alanine at position 329 in VP1 ORF (dominant mutation Thr329Ala), was detected in a single sequence belonging to a reassortant isolate (IBD13HeB01).

## DISCUSSION

The present study investigates the evolution by serial passaging of two genetically homogeneous virus stocks generated by reverse

genetics from infectious clones representing two IBDV viral strains (an attenuated classical virulent, rCu-1, in chicken B cells and DF-1 cells and a very virulent strain, rrv, in only chicken B cells) with and without a selection pressure imposed using the antiviral bases analog 7DMA. It also investigates the pathogenicity of passaged rrv in chickens.

## A Higher Mutation Frequency and Nucleotide Diversity Was Generated in Segment A Than in Segment B, Regardless 7DMA Treatment and Viral Strain

The increase in mutation frequency and genetic diversity can help viruses to adapt to new environments, but this needs to be in compromise with genetic information conservation. In this concern, an important remark to maintain IBDV genetic integrity is the upper limit in mutation frequency that may be tolerated by IBDV. In the present study, the highest mutation frequency value was observed in segment A from rrv-p12/BF (27.6 mutations/10<sup>4</sup> nt), mainly due to mutations occurring in VP2 and VP3 CDRs. In segment B, the highest values were always reached under 7DMA treatment, with an upper limit on mutation frequency in the range of 11.8–15.9 mutations/10<sup>4</sup> nt. Similar values to that one found in segment B were observed in CVB3 low fidelity variants (Gnadig et al., 2012), which were considered to be very high mutation frequencies. The increase in viral diversity, determined through nucleotide diversity ( $\pi$ ), from p0 to p12 in cells or p0 to p5 in chickens in both segments and in both viruses (with exception for rCu-1-p12/DF-1 in segment B) was expected, since genetically homogeneous virus stocks generated by reverse genetics were used in p0. A similar expansion in viral diversity was previously observed in a Coxsackie virus B3 (CVB3) clone recovered from an infectious cDNA plasmid and serially passaged in two immortalized cell lines (Borderia et al., 2015). Again, segment A showed the most genetic diversity, where the highest values were reached by rCu-1-p12/B and rCu-1-p12/B/7DMA. Why these values were higher in chicken B cells than in DF-1 cells could be explained by a stronger bottleneck effect, driven maybe by a lower MOI used in chicken B cells than in DF-1 cells. Recently, a study on rhesus rotavirus populations indicated a positive correlation between the increase of the genetic diversity and a lower MOI (Kadoya et al., 2020). However, it happened only for segment A, while the values for segment B were similar regardless the presence of 7DMA, the virus strain or the biological system used, suggesting a lower genetic plasticity of segment B. This fact could indicate that, at least in segment A, rCu-1 evolution is cell type-dependent. Therefore, the maximum complexity of a mutant spectrum was reached in segment A, especially when rCu-1 was passaged.

A possible explanation for the high values in genetic diversity and mutant frequency in segment A and for rCu-1 could be the increase in rCu-1 replicative fitness in comparison with rrv, which is characterized by its already high fitness, as documented by high viral loads in the BF upon *in vivo* infection (Le Nouen et al., 2012). The Ile74Phe, Thr131Ala, Arg133Trp mutations in VP5, Cys680Tyr mutation in VP4 and U3205C change in 3'UTR,

could support this assumption since the residues Phe74, Ala131 and Trp133 in VP5, Tyr680 in VP4 and C3205 in the 3'UTR are present in vvIBDV strains (this assumption is further discussed in section 4.3).

These results show, for the first time, the increase in IBDV genetic diversity in response to selection pressures.

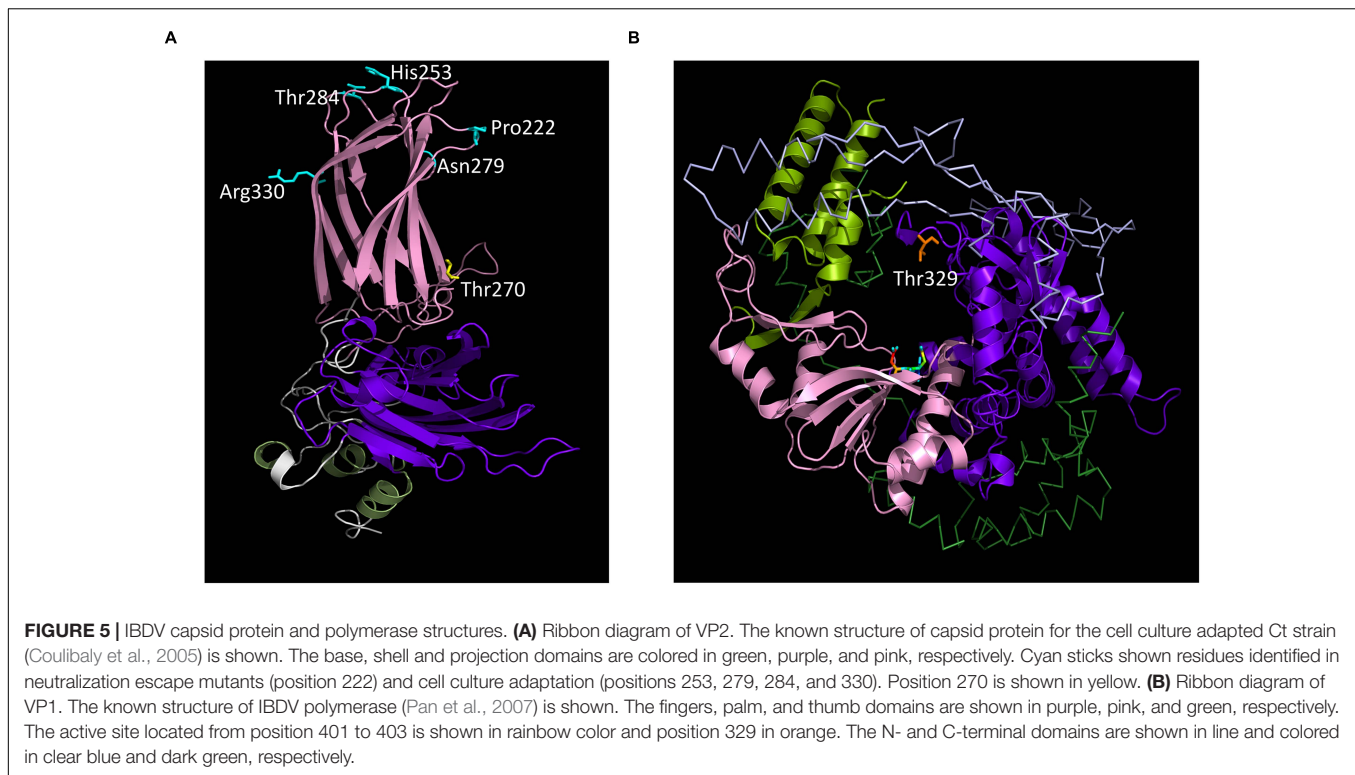
## Chicken B Cells Did Not Select Known VP2 Mutations Associated to Cell Culture Adaptation in rrv

Many cell culture systems have been used in the study of IBDV. Most of these systems carry the inconvenience that they require modifications in hVP2, especially for non-cell culture adapted viruses, resulting in their attenuation *in vivo*. The rescue of rrv-p0 was recently carried out successfully in primary chicken B cells without modification in hVP2 (which spans from positions 206 to 350) (Cubas-Gaona et al., 2020) as evaluated by Sanger sequencing and confirmed in the present study by NGS.

Here, 12 passages of rrv-p0 in chicken B cells did not lead, in spite of an increased genetic diversity compared to rrv-p0, to the apparition of mutations in VP2 positions 253, 279, 284 or 330 previously described as required for *in vitro* cell culture adaptation and/or altering the virulence *in vivo*. However, VP2 Ala270Glu or Ala270Thr mutations, which are also located into hVP2, were detected as dominant mutations in rrv-p12 and rrv-p12/7DMA, respectively. Unlike positions 253, 279, 284 or 330, VP2 position 270 is located at the base of the projection domain (P) (Figure 5A), one of the three domains present in VP2 (Coulibaly et al., 2005). The VP2 Ala270Glu mutation has been previously observed in two vvIBDV strains (OKYM and DV86) after three passages in DT40 cells, an avian leukosis virus-induced chicken B cell line (Terasaki et al., 2008). In addition, glutamic acid in position 270 of VP2 has been reported in another vvIBDV strain which produced low mortality rate (Hoque et al., 2001), suggesting a possible role of this amino acid in the pathogenesis in chickens. Therefore, this mutation may contribute to the reduction in mortality (although not statistically significant in the present study) in chickens infected with rrv-p12. Ala222Val, another substitution in hVP2, was present in the three replicates in rrv-p12, at low variant frequencies (10, 11 and 13%) and persisted after infection *in vivo*. Although position 222 is well exposed at the top of VP2, no available information exists about its role in cell culture adaptation and virulence changes, but this position has been identified as contributing to IBDV antigenicity (Schnitzler et al., 1993; Eterradossi et al., 1997; Samy et al., 2020). Further studies are needed to confirm the role of mutations at VP2 positions 222 and 270. In particular, it is unclear if one or both the dominant mutations detected in rrv-p12, namely VP2 Ala270Thr and/or the mutation in segment B 3'UTR, have an impact on viral phenotype.

## rCu-1 Passage in B Cells Partially Mirrors *in vivo* Evolution

Two mutations were detected in rCu-1-p0 at low frequencies (below 10%). These mutations were not found after 12 passages in chicken B cells nor after 5 passages in chickens, which indicates



that these mutations were transient. Since the rCu-1-p0 sequence used in the present study was based on a cell culture adapted Cu-1 strain (Nick et al., 1976), reversion from histidine to glutamine (wild-type residue) at position 253 was expected after passages. Mutations in VP2 at position 253, such as, in most cases, His253Gln, but also His253Asn or His253Asp were indeed observed in vaccine-related viruses isolated from chickens in the field (Olesen et al., 2018). However, in the present study, passages in chickens promoted the apparition of a leucine instead of a glutamine at position 253 in 100% of the viral population, while histidine 253 remained stable in chicken B cells and DF-1 cells. Analysis of complete IBDV genomes available in Genbank revealed that this 253Leu residue was not previously reported. The impact of this residue on viral properties deserves further studies. The lack of mutation of rCu-1 in VP2 position 253 after passages in B cells indicates that additional constraints, present *in vivo*, are required to select changes in this position. In this aspect, chicken B cells did not mirror IBDV evolution *in vivo*.

Surprisingly, the study of IBDV sequences from Genbank revealed the strict conservation of a threonine in position 713 in VP4. The presence of an Alanine at position 713 thus appears as a uniqueness of the rCu-1 sequence used in the present study. It nevertheless illustrates how interesting is the use of chicken B cells, since reversion to a threonine was observed in both those cells and in chickens, but not in DF-1 cells.

Although the Cys680Tyr mutation was only found in chicken B cells and DF-1 cells passaged rCu-1, this position has acquired relevance by belonging, together with four others residues to a VP4 genetic signature of virulence. Recently, Dulwich et al. (2020) demonstrated that VP4 antagonizes type I IFN induction

in a strain-dependent manner. Specifically, vvIBDV strains, which harbor a tyrosine in this position, possess an enhanced ability in IFN antagonism compared with classical viruses, which have a cysteine in this position. It is thus tempting to speculate that the acquisition of this change in rCu-1 could promote higher viral fitness, by better inhibiting innate immunity. However, why this was not observed for rCu-1 passaged in chickens remains an open question. During *in vivo* passaging, in spite of the nearly 100 fold increase of the mean viral titer in the bursae, chickens did not develop any clinical sign, which indicates that mutations that arose during the *in vivo* passages are not sufficient to render the virus pathogenic. Further work, using reverse genetics, is necessary to dissect which mutations contribute to this increased replicative fitness *in vivo* and whether this goes with microscopic lesions of the bursa or immunosuppression.

Finally, the U3205C change, located in the 3'UTR sequence of segment A, found exclusively in rCu-1-p12/B/7DMA, is highly conserved in vvIBDV strains (Xia et al., 2008). This mutation could provoke changes in the RNA secondary structure and enhance the virulence as previously suggested (Xia et al., 2008).

### VP1 Thr329Ala in IBDV Viral Polymerase Together With VP2 Ala270Thr Could Be Responsible for the Reduced Pathogenicity Provoked by rvv-p12/7DMA

Alteration of viral polymerase fidelity has allowed a better understanding of viral evolution and adaptation (Pfeiffer and Kirkegaard, 2003; Coffey and Vignuzzi, 2010;

Gnadig et al., 2012). Nucleoside analogs, such as ribavirin and 5-fluorouracil, have been classically used as a selective pressure in order to select viral resistant mutants (Borderia et al., 2016). The inhibitory effect of 7DMA on IBDV replication was previously addressed (Cubas-Gaona et al., 2018). In the present study, the detection in p12 of a unique non-synonymous and dominant mutation, VP1 Thr329Ala in segment B of both rvv and rCu-1 and in both chicken B cells and DF-1 cells, suggested that a resistance mechanism was established throughout the passages to overcome the mutagenic effects of 7DMA. Deep-sequencing of the intermediate viral stocks would be necessary to thoroughly address this point; this approach is beyond the scope of this study whose objective was to identify relevant mutations in the final viral stocks.

The alignment results indicated that Thr329 is present in 147 out of 152 published segment B sequences in NCBI database, which suggests this residue is highly conserved and important during viral genome replication and transcription. IBDV polymerase contains fingers, palm and thumb subdomains and, as most polymerases, has the shape of a right hand (Pan et al., 2007). Thr329 is located inside the finger subdomain in a 15-residue loop (residues 321–335) forming a fingertip structure (Pan et al., 2007), which is a unique feature of RdRps. This structure helps to form template-binding and NTP channels through which NTPs would reach the active site (Choi, 2012). In **Figure 5B**, residue Thr329 is shown (in orange), which appears distant from the active site residues (in rainbow color). Similar locations for mutations, in finger subdomain, were detected in other viral high-fidelity, nucleoside analog ribavirin-resistant polymerases, such as Gly64 in poliovirus (Pfeiffer and Kirkegaard, 2003) and Leu123 in Human enterovirus 71 (Meng and Kwang, 2014).

During chicken infection, carried out in absence of 7DMA, rvv-p12/7DMA/BF viral population showed to be the most genetically heterogeneous in segment B, with a stable Thr329Ala mutation. Therefore, the *in vivo* attenuation of rvv-p12/7DMA, shown by the significant reduction in mortality rate in spite of otherwise unchanged phenotypic traits (such as viral titer in BF, b/B ratio, bursal atrophy and blood B cells depletion), could be the result of its more diverse genetic population harboring an increased percentage of genomes with reduced viral fitness. This fact could compromise viral replication and dissemination, and together with Ala270Thr mutation in VP2 contribute to the observed *in vivo* attenuation. This population with lower fitness could be the main reason whereby viral shedding in the rvv-p12/7DMA group was lower at 3 and 4 d.p.i. compared with that of the other rvv groups. Similarly, the statistically significant splenomegaly at 4 d.p.i. in the rvv-p12/7DMA group may be due to this high genetic diversity and/or to a reduced replicative fitness leading to a higher activation of the inflammatory response.

In conclusion, this work, through the use of genetically homogeneous virus stocks, illustrates the evolution of IBDV in various host systems. In these conditions, segment A showed the highest genetic variation. The various dominant changes identified in this study such as His253Leu, Ala270Glu and Ala270Thr in VP2, Cys680Tyr in

VP4 and Thr329Ala in VP1 represent candidate virulence markers and merit further investigation using IBDV reverse genetics.

This study illustrates also how NGS sheds new light on the existence of minority mutants, which may have been unnoticed in previous studies relying on Sanger sequencing; these mutations may modulate viral proteins properties and may contribute to shape viral phenotypes.

## DATA AVAILABILITY STATEMENT

The data presented in the study are deposited in the BioSample database at NCBI under accession numbers from SAMN14642839 to SAMN14642909. The data is publicly available.

## ETHICS STATEMENT

All animal trials were conducted in an animal facility approved for animal experiments (n° C-22-745-1) and were approved by ANSES Ploufragan local committee for animal welfare; chickens were raised and humanely euthanized in agreement with EU directive number 2010/63/UE. Serial passages of rCu-1-p0 in chickens were approved by ANSES Ethical Committee, registered at the national level under number C2EA-016/ComEth ANSES/ENVA/UPEC and authorized by French Ministry for higher education and research under permit number APAFiS#2494-201512021054584v1. Pathogenicity assessment in SPF chickens was approved by ANSES Ethical Committee, registered at the national level under number C2EA-016/ComEth ANSES/ENVA/UPEC and authorized by French Ministry for higher education and research under permit number APAFiS#4945-2016041316546318 v6.

## AUTHOR CONTRIBUTIONS

LLC-G carried out experiments, analyzed the results, and wrote the manuscript. AF analyzed the data from NGS. LLC-G, CC, and SS carried out the animal experiments. CC analyzed blood samples by flow cytometry. F-XB carried out the analysis of mutations present IBDV genomes from databases. MC modeled the non-coding regions. SB gave support in the statistical analysis. YB, PL, HQ, and AL carried out the NGS. PL carried out BioSample submission. MA supervised technically the animal experiment. NE, BG, PAB, and AK revised the manuscript. SS conceived the study, supervised LLC-G and CC and revised the manuscript. All authors contributed to the article and approved the submitted version.

## FUNDING

LLC-G received a post-doctoral fellowship from “Région Bretagne” (program “Stratégie D’Attractivité Durable,” Grant

Number 17002) and “Agglomération de Saint-Brieuc.” This study received funding from the European Union’s Horizon 2020 (VetBioNet) research and innovation program under grant agreement N° 731014.

## ACKNOWLEDGMENTS

The authors would like to thank to Dolores Rodriguez Aguirre and Francisco Rodriguez Aguirre from Centro Nacional de Biotecnología (CNB-CSIC, Madrid-Spain) for their kind help during the design of the first part of passaging protocol and to Bernd Kaspers and Sonja Härtle from The University of Munich (Munich-Germany) for their critical opinion in the analysis of white blood cell counting.

## REFERENCES

- Abed, M., Soubies, S., Courtyllon, C., Briand, F. X., Allee, C., Amelot, M., et al. (2018). Infectious bursal disease virus in Algeria: detection of highly pathogenic reassortant viruses. *Infect. Genet. Evol.* 60, 48–57. doi: 10.1016/j.meegid.2018.01.029
- Bayliss, C. D., Spies, U., Shaw, K., Peters, R. W., Papageorgiou, A., Müller, H., et al. (1990). A comparison of the sequences of segment a of four infectious bursal disease virus strains and identification of a variable region in VP2. *J. Gen. Virol.* 71(Pt 6), 1303–1312. doi: 10.1099/0022-1317-71-6-1303
- Beaucourt, S., Borderia, A. V., Coffey, L. L., Gnädig, N. F., Sanz-Ramos, M., Beeharry, Y., et al. (2011). Isolation of fidelity variants of RNA viruses and characterization of virus mutation frequency. *J. Vis. Exp.* 52:2953. doi: 10.3791/2953
- Boot, H. J., and Pritz-Verschuren, S. B. (2004). Modifications of the 3′-UTR stem-loop of infectious bursal disease virus are allowed without influencing replication or virulence. *Nucleic Acids Res.* 32, 211–222. doi: 10.1093/nar/gkh177
- Borderia, A. V., Isakov, O., Moratorio, G., Henningson, R., Aguera-Gonzalez, S., Organtini, L., et al. (2015). Group selection and contribution of minority variants during virus adaptation determines virus fitness and phenotype. *PLoS Pathog* 11:e1004838. doi: 10.1371/journal.ppat.1004838
- Borderia, A. V., Rozen-Gagnon, K., and Vignuzzi, M. (2016). Fidelity variants and RNA quasispecies. *Curr. Top. Microbiol. Immunol.* 392, 303–322. doi: 10.1007/82\_2015\_483
- Chettle, N., Stuart, J. C., and Wyeth, P. J. (1989). Outbreak of virulent infectious bursal disease in East Anglia. *Vet. Rec.* 125, 271–272. doi: 10.1136/vr.125.10.271
- Cheung, P. P., Watson, S. J., Choy, K. T., Fun Sia, S., Wong, D. D., Poon, L. L., et al. (2014). Generation and characterization of influenza A viruses with altered polymerase fidelity. *Nat. Commun.* 5:4794. doi: 10.1038/ncomms5794
- Choi, K. H. (2012). Viral polymerases. *Adv. Exp. Med. Biol.* 726, 267–304. doi: 10.1007/978-1-4614-0980-9\_12
- Coffey, L. L., and Vignuzzi, M. (2010). Host alternation of Chikungunya virus increases fitness while restricting population diversity and adaptability to novel selective pressures. *J. Virol.* 85, 1025–1035. doi: 10.1128/jvi.01918-10
- Cosgrove, A. S. (1962). An apparently new disease of chickens: avian nephrosis. *Avian Dis.* 6, 385–389. doi: 10.2307/1587909
- Coulbaly, F., Chevalier, C., Gutsche, I., Pous, J., Navaza, J., Bressanelli, S., et al. (2005). The birnavirus crystal structure reveals structural relationships among icosahedral viruses. *Cell* 120, 761–772. doi: 10.1016/j.cell.2005.01.009
- Crotty, S., Maag, D., Arnold, J. J., Zhong, W., Lau, J. Y., Hong, Z., et al. (2000). The broad-spectrum antiviral ribonucleoside ribavirin is an RNA virus mutagen. *Nat. Med.* 6, 1375–1379. doi: 10.1038/82191
- Cubas-Gaona, L. L., Diaz-Beneitez, E., Ciscar, M., Rodriguez, J. F., and Rodriguez, D. (2018). Exacerbated apoptosis of cells infected with infectious bursal disease

## SUPPLEMENTARY MATERIAL

The Supplementary Material for this article can be found online at: <https://www.frontiersin.org/articles/10.3389/fmicb.2021.678563/full#supplementary-material>

**Supplementary Figure 1** | Gating strategy used for the identification of thrombocytes (CD45<sup>+</sup> K1<sup>+</sup>), monocytes (CD45<sup>+</sup> K1<sup>+</sup>Kul01<sup>+</sup>), chicken B cells (CD45<sup>+</sup> Bu1<sup>+</sup>), and T-cells (CD45<sup>+</sup> CD4<sup>+</sup>, CD45<sup>+</sup>CD8<sup>+</sup> and CD45 TCRγδ<sup>+</sup>) based on marker expression followed by FSC/SSC characteristics.

**Supplementary Figure 2** | Blood counts of T cells, thrombocytes and monocytes in chickens infected with rvv-p0, rvv-p12, or rvv-p12/7DMA. Cell concentrations in blood at 2 and 21 days post-inoculation (d.p.i.) (n = 10 chickens per group except for the rvv-p0 group). Points represent individual values; boxplots indicate median and interquartile range. For all graphs, different letters indicate a p-value < 0.05 between the different groups using Kruskal-Wallis test followed by Fisher’s least significant difference test with Holm adjustment method for multiple comparisons. NI, non-infected group.

- virus upon exposure to interferon alpha. *J. Virol.* 92:e00364-18. doi: 10.1128/JVI.00364-18
- Cubas-Gaona, L. L., Trombetta, R., Courtyllon, C., Li, K., Qi, X., Wang, X., et al. (2020). Ex vivo rescue of recombinant very virulent IBDV using a RNA polymerase II driven system and primary chicken bursal cells. *Sci. Rep.* 10:13298. doi: 10.1038/s41598-020-70095-x
- Dey, S., Pathak, D. C., Ramamurthy, N., Maity, H. K., and Chellappa, M. M. (2019). Infectious bursal disease virus in chickens: prevalence, impact, and management strategies. *Vet. Med. (Auckl.)* 10, 85–97. doi: 10.2147/VMRR.S185159
- Domingo, E., and Perales, C. (2019). Viral quasispecies. *PLoS Genet.* 15:e1008271. doi: 10.1371/journal.pgen.1008271
- Dulwich, K. L., Asfor, A., Gray, A., Giotis, E. S., Skinner, M. A., and Broadbent, A. J. (2020). The stronger downregulation of in vitro and in vivo innate antiviral responses by a very virulent strain of infectious bursal disease virus (IBDV), compared to a classical strain, is mediated, in part, by the VP4 protein. *Front. Cell Infect. Microbiol.* 10:315. doi: 10.3389/fcimb.2020.00315
- Eigen, M. (2002). Error catastrophe and antiviral strategy. *Proc. Natl. Acad. Sci. U.S.A.* 99, 13374–13376. doi: 10.1073/pnas.212514799
- Escaffre, O., Queguiner, M., and Eterradossi, N. (2010). Development and validation of four Real-Time quantitative RT-PCRs specific for the positive or negative strands of a bisegmented dsRNA viral genome. *J. Virol. Methods* 170, 1–8. doi: 10.1016/j.jviromet.2010.07.009
- Eterradossi, N., Picault, J. P., Drouin, P., Guittet, M., L’Hospitalier, R., and Bennejan, G. (1992). Pathogenicity and preliminary antigenic characterization of six infectious bursal disease virus strains isolated in France from acute outbreaks. *Zentralbl. Veterinarmed. B* 39, 683–691. doi: 10.1111/j.1439-0450.1992.tb01222.x
- Eterradossi, N., and Saif, Y. M. (2020). *Infectious Bursal Disease*. Hoboken, NJ: Wiley-Blackwell.
- Eterradossi, N., Toquin, D., Rivallan, G., and Guittet, M. (1997). Modified activity of a VP2-located neutralizing epitope on various vaccine, pathogenic and hypervirulent strains of infectious bursal disease virus. *Arch. Virol.* 142, 255–270. doi: 10.1007/s007050050075
- Flageul, A., Lucas, P., Hirchaud, E., Touzain, F., Blanchard, Y., Eterradossi, N., et al. (2021). Viral variant visualizer (VVV): a novel bioinformatic tool for rapid and simple visualization of viral genetic diversity. *Virus Res.* 291:198201. doi: 10.1016/j.virusres.2020.198201
- Gnädig, N. F., Beaucourt, S., Campagnola, G., Borderia, A. V., Sanz-Ramos, M., Gong, P., et al. (2012). Coxsackievirus B3 mutator strains are attenuated in vivo. *Proc. Natl. Acad. Sci. U.S.A.* 109, E2294–E2303. doi: 10.1073/pnas.1204022109
- Hall, R. J., Wang, J., Todd, A. K., Bissielo, A. B., Yen, S., Strydom, H., et al. (2014). Evaluation of rapid and simple techniques for the enrichment of viruses prior to metagenomic virus discovery. *J. Virol. Methods* 195, 194–204. doi: 10.1016/j.jviromet.2013.08.035

- Hoque, M. M., Omar, A. R., Chong, L. K., Hair-Bejo, M., and Aini, I. (2001). Pathogenicity of SspI-positive infectious bursal disease virus and molecular characterization of the VP2 hypervariable region. *Avian Pathol.* 30, 369–380. doi: 10.1080/03079450120066377
- Jackwood, D. H., and Saif, Y. M. (1987). Antigenic diversity of infectious bursal disease viruses. *Avian Dis.* 31, 766–770.
- James, K. T., Cooney, B., Agopowicz, K., Trevors, M. A., Mohamed, A., Stoltz, D., et al. (2016). Novel high-throughput approach for purification of infectious virions. *Sci. Rep.* 6:36826. doi: 10.1038/srep36826
- Kadoya, S.-S., Urayama, S.-I., Nunoura, T., Hirai, M., Takaki, Y., Kitajima, M., et al. (2020). Bottleneck size-dependent changes in the genetic diversity and specific growth rate of a rotavirus a strain. *J. Virol.* 94:e02083-19. doi: 10.1128/jvi.02083-19
- Le Nouen, C., Toquin, D., Muller, H., Raue, R., Kean, K. M., Langlois, P., et al. (2012). Different domains of the RNA polymerase of infectious bursal disease virus contribute to virulence. *PLoS One* 7:e28064. doi: 10.1371/journal.pone.0028064
- Levi, L. I., Gnadig, N. F., Beaucourt, S., McPherson, M. J., Baron, B., Arnold, J. J., et al. (2010). Fidelity variants of RNA dependent RNA polymerases uncover an indirect, mutagenic activity of amiloride compounds. *PLoS Pathog.* 6:e1001163. doi: 10.1371/journal.ppat.1001163
- Lim, B. L., Cao, Y., Yu, T., and Mo, C. W. (1999). Adaptation of very virulent infectious bursal disease virus to chicken embryonic fibroblasts by site-directed mutagenesis of residues 279 and 284 of viral coat protein VP2. *J. Virol.* 73, 2854–2862.
- McFerran, J. B., McNulty, M. S., McKillop, E. R., Connor, T. J., McCracken, R. M., Collins, D. S., et al. (1980). Isolation and serological studies with infectious bursal disease viruses from fowl, turkeys and ducks: demonstration of a second serotype. *Avian Pathol.* 9, 395–404. doi: 10.1080/03079458008418423
- Meng, T., and Kwang, J. (2014). Attenuation of human enterovirus 71 high-replication-fidelity variants in AG129 mice. *J. Virol.* 88, 5803–5815. doi: 10.1128/JVI.00289-14
- Nick, H., Cursiefen, D., and Becht, H. (1976). Structural and growth characteristics of infectious bursal disease virus. *J. Virol.* 18, 227–234.
- Noor, M., Mahmud, M. S., Ghose, P. R., Roy, U., Nooruzzaman, M., Chowdhury, E. H., et al. (2014). Further evidence for the association of distinct amino acid residues with in vitro and in vivo growth of infectious bursal disease virus. *Arch. Virol.* 159, 701–709. doi: 10.1007/s00705-013-1885-2
- Olesen, L., Dijkman, R., Koopman, R., van Leeuwen, R., Gardin, Y., Dwars, R. M., et al. (2018). Field and laboratory findings following the large-scale use of intermediate type infectious bursal disease vaccines in Denmark. *Avian Pathol.* 47, 595–606. doi: 10.1080/03079457.2018.1520388
- Olsen, D. B., Eldrup, A. B., Bartholomew, L., Bhat, B., Bosserman, M. R., Ceccacci, A., et al. (2004). A 7-Deaza-adenosine analog is a potent and selective inhibitor of hepatitis C virus replication with excellent pharmacokinetic properties. *Antimicrob. Agents Chemother.* 48, 3944–3953. doi: 10.1128/aac.48.10.3944-3953.2004
- Pan, J., Vakharia, V. N., and Tao, Y. J. (2007). The structure of a birnavirus polymerase reveals a distinct active site topology. *Proc. Natl. Acad. Sci. U.S.A.* 104, 7385–7390. doi: 10.1073/pnas.0611599104
- Pfeiffer, J. K., and Kirkegaard, K. (2003). A single mutation in poliovirus RNA-dependent RNA polymerase confers resistance to mutagenic nucleotide analogs via increased fidelity. *Proc. Natl. Acad. Sci. U.S.A.* 100, 7289–7294. doi: 10.1073/pnas.1232294100
- Reed, L. J., and Muench, H. (1938). A simple method of estimating fifty per cent endpoints. *Am. J. Epidemiol.* 27, 493–497. doi: 10.1093/oxfordjournals.aje.a118408
- Samy, A., Courtillon, C., Briand, F. X., Khalifa, M., Selim, A., Arafa, A. E. S., et al. (2020). Continuous circulation of an antigenically modified very virulent infectious bursal disease virus for fifteen years in Egypt. *Infect. Genet. Evol.* 78:104099. doi: 10.1016/j.meegid.2019.104099
- Schnitzler, D., Bernstein, F., Muller, H., and Becht, H. (1993). The genetic basis for the antigenicity of the VP2 protein of the infectious bursal disease virus. *J. Gen. Virol.* 74(Pt 8), 1563–1571. doi: 10.1099/0022-1317-74-8-1563
- Seliger, C., Schaerer, B., Kohn, M., Pendl, H., Weigend, S., Kaspers, B., et al. (2012). A rapid high-precision flow cytometry based technique for total white blood cell counting in chickens. *Vet. Immunol. Immunopathol.* 145, 86–99. doi: 10.1016/j.vetimm.2011.10.010
- Song, L., Huang, W., Kang, J., Huang, Y., Ren, H., and Ding, K. (2017). Comparison of error correction algorithms for Ion Torrent PGM data: application to hepatitis B virus. *Sci. Rep.* 7:8106. doi: 10.1038/s41598-017-08139-y
- Soubies, S. M., Courtillon, C., Abed, M., Amelot, M., Keita, A., Broadbent, A., et al. (2018). Propagation and titration of infectious bursal disease virus, including non-cell-culture-adapted strains, using ex vivo-stimulated chicken bursal cells. *Avian Pathol.* 47, 179–188. doi: 10.1080/03079457.2017.1393044
- Terasaki, K., Hirayama, H., Kasanga, C. J., Maw, M. T., Ohya, K., Yamaguchi, T., et al. (2008). Chicken B lymphoma DT40 cells as a useful tool for in vitro analysis of pathogenic infectious bursal disease virus. *J. Vet. Med. Sci.* 70, 407–410. doi: 10.1292/jvms.70.407
- van Loon, A. A., de Haas, N., Zeyda, I., and Mundt, E. (2002). Alteration of amino acids in VP2 of very virulent infectious bursal disease virus results in tissue culture adaptation and attenuation in chickens. *J. Gen. Virol.* 83(Pt 1), 121–129. doi: 10.1099/0022-1317-83-1-121
- Van Slyke, G. A., Arnold, J. J., Lugo, A. J., Griesemer, S. B., Moustafa, I. M., Kramer, L. D., et al. (2015). Sequence-specific fidelity alterations associated with west Nile virus attenuation in mosquitoes. *PLoS Pathog.* 11:e1005009. doi: 10.1371/journal.ppat.1005009
- Xia, R. X., Wang, H. Y., Huang, G. M., and Zhang, M. F. (2008). Sequence and phylogenetic analysis of a Chinese very virulent infectious bursal disease virus. *Arch. Virol.* 153, 1725–1729. doi: 10.1007/s00705-008-0140-8
- Zeng, J., Wang, H., Xie, X., Yang, D., Zhou, G., and Yu, L. (2013). An increased replication fidelity mutant of foot-and-mouth disease virus retains fitness in vitro and virulence in vivo. *Antiviral Res.* 100, 1–7. doi: 10.1016/j.antiviral.2013.07.008
- Zhao, L., and Illingworth, C. J. R. (2019). Measurements of intrahost viral diversity require an unbiased diversity metric. *Virus Evol.* 5:vey041. doi: 10.1093/ve/vey041
- Zmurko, J., Marques, R. E., Schols, D., Verbeke, E., Kaptein, S. J., and Neyts, J. (2016). The viral polymerase inhibitor 7-Deaza-2'-C-methyladenosine is a potent inhibitor of in vitro zika virus replication and delays disease progression in a robust mouse infection model. *PLoS Negl. Trop. Dis.* 10:e0004695. doi: 10.1371/journal.pntd.0004695
- Zuker, M. (2003). Mfold web server for nucleic acid folding and hybridization prediction. *Nucleic Acids Res.* 31, 3406–3415. doi: 10.1093/nar/gkg595

**Conflict of Interest:** The authors declare that the research was conducted in the absence of any commercial or financial relationships that could be construed as a potential conflict of interest.

Copyright © 2021 Cubas-Gaona, Flageul, Courtillon, Briand, Contrant, Bougeard, Lucas, Quenault, Leroux, Keita, Amelot, Grasland, Blanchard, Etrradossi, Brown and Soubies. This is an open-access article distributed under the terms of the Creative Commons Attribution License (CC BY). The use, distribution or reproduction in other forums is permitted, provided the original author(s) and the copyright owner(s) are credited and that the original publication in this journal is cited, in accordance with accepted academic practice. No use, distribution or reproduction is permitted which does not comply with these terms.